

Luminosity Functions of Type Ia Supernovae and their Host Galaxies from the Sloan Digital Sky Survey

Naoki Yasuda^{1,3} and Masataka Fukugita^{1,2,3}

¹*Institute for Cosmic Ray Research, University of Tokyo, Kashiwa 277-8582, Japan*

²*Institute for Advanced Study, Princeton, NJ08540, U.S.A.*

³*Institute for the Physics and Mathematics of the Universe, University of Tokyo, Kashiwa 277-8568, Japan*

ABSTRACT

The sample of 137 low-redshift type Ia supernovae with $0.05 \leq z \leq 0.3$ obtained from the SDSS-II Supernova Survey for the southern equatorial stripe of 300 square degrees is used to derive the luminosity functions of type Ia supernovae and of their host galaxies in the *gri* passbands. We show that the luminosity function of type Ia supernova host galaxies matches well with that of galaxies in the general field, suggesting that the occurrence of type Ia supernovae does not favour a particular type of galaxies but is predominantly proportional to the luminosity of galaxies. The evidence is weak that the supernovae rate varies with colour of host galaxies. The only evidence that points to possible correlation between the supernova rate and star formation activity is that the supernova rate in late-type galaxies is higher than that in early-type galaxies by $31 \pm 35\%$. In our low redshift sample the component of type Ia supernova rate that is proportional to star formation activity is not manifest in the integrated supernova rate, while our observation is compatible with the current two-component models. The sample contains 8 type Ia supernovae whose host galaxies were not identified, but it is shown that their occurrence is consistent with them occurred in low luminous galaxies beyond the survey. The luminosity function of type Ia supernovae is approximately Gaussian with the full-width half maximum being a factor of 1.4 in luminosity. The Gaussian distribution becomes tighter if the ratio of extinction to reddening, R_V , is lower than the characteristic value for the Milky Way and if luminosity is corrected for the light curve shape. The colour excess is ≈ 0.07 mag which is significantly smaller than reddening expected for field galaxies. This colour excess does not vary with the distance of the supernovae from the centre of the host galaxy to 15 kpc. This suggests that the major part of the colour excess appears to be either intrinsic or reddening that arises in the immediate environment of supernova, rather than interstellar reddening in host galaxies, and most of type Ia supernovae take place in relatively dust free environment.

Subject headings: supernovae : general

1. Introduction

Recent studies have revealed that our understanding of the mechanism of Type Ia supernovae (SNe Ia) is poorer than we had thought. It is suspected that there are two different progenitor types responsible for SNe Ia: explosions from old systems as in the long-accepted scenario and explosions in young stellar systems (Dallaporta 1973; Tammann 1982; Mannucci et al. 2005; Sullivan et al. 2006). The evidence, however, is not conclusive yet, and some observations at high redshift do not fit this picture; for example, there are indications for a drop in the SN rate at $z > 1.5$, where star formation rate is still rising (Poznanski et al. 2007; Dahlen et al. 2008), which does not support the presence of a large prompt component.

The present paper studies the luminosity functions (LF) of SNe Ia and their host galaxies and correlations in properties of SN Ia and of host galaxies. Miller & Branch (1990) and Richardson et al. (2002) studied the LF of various types of SNe based on the Asiago Supernova Catalog (Barbon et al. 1989). In particular, Richardson et al. (2002) showed that the LF of SNe Ia is consistent with the Gaussian distribution with $\langle M_B \rangle = -19.46 + 5 \log(H_0/60)$ and $\sigma = 0.56$ using 111 spectroscopically normal SNe Ia without correcting for the light curve shape parameter. With the correction for the decline rate σ can be reduced to 0.11 (Phillips 1999). We are not aware of a study of the LF of SNe Ia host galaxies. We may hope that a comparison with the LF of field galaxies may hint us as to what type of galaxies would preferentially host SNe Ia.

We have accumulated a sample of SNe Ia acquired in the second phase of the Sloan Digital Sky Survey (SDSS; York et al. 2000). Supernovae were searched during September to November of 2005 to 2007 by repeated imaging for the sky area of 300 square degree of the southern equatorial region, $-60^\circ < \text{R.A.} < +60^\circ$, $-1^\circ.25 < \text{Decl.} < +1^\circ.25$, every two days (Frieman et al. 2008; Sako et al. 2008; Dilday et al. 2008). Approximately 500 SNe Ia at $0.05 < z < 0.4$ were identified using well-defined selection criteria and their light curves were measured (Sako et al. 2008; Holtzman et al. 2008). The advantage of the use of the SDSS is, apart from its accurate five colour photometry (Fukugita et al. 1996; Smith et al. 2002), that most of the galaxies that host supernovae have already been photometrically observed with homogeneous presetted criteria, so that one can study the properties of those galaxies and correlations between the supernovae and their host galaxies. The disadvantage is that the SDSS is somewhat too shallow for this purpose due to a limitation arising from the time-delay-and-integrate mode imaging with the 2.5 m aperture telescope (Gunn et al. 1998, 2006).

The SN candidates are spectroscopically followed-up with other telescopes as much as the time allows to determine their types and redshifts (Zheng et al. 2008). After the SN light faded away spectroscopic observations are carried out for its host galaxy to determine redshift of the SN Ia candidate. In this paper we use the data from the first year for the completeness is high for redshift of host galaxies for the first year SNe. We limit the sample effectively to $z \lesssim 0.3$ for the sample completeness. Five colour photometry had been made for host galaxies. A $0.1L^*$ galaxy at $z \approx 0.3$ would give $g \sim 22.7$, $r \sim 21.9$, $i \sim 21.4$, $z \sim 21.1$, so that we can sustain reasonable accuracy in

SDSS photometry for the four passbands (Hogg et al. 2001; Ivezić et al. 2004). For the u passband, however, a $0.1L^*$ galaxy at $z \approx 0.3$ gives $u \sim 24.3$, which is significantly beyond our survey limit $u = 22.0$, a calibre of our survey with a 2.5-m telescope, and hence, the u passband information cannot efficiently be exploited.

In this paper, we take $H_0 = 70 \text{ km s}^{-1} \text{ Mpc}^{-1}$, $\Omega_m = 0.3$ and $\Omega_\Lambda = 0.7$ for the cosmological parameters.

2. Sample

In the 2005 SDSS-II observation, 706 SNe Ia candidates were identified including objects with observations at only a few epochs and 130 SNe Ia among them are spectroscopically confirmed with additional 16 identified as spectroscopically probable SNe Ia. The latter are the objects whose spectrum do not show significant Si II absorption-line feature while the overall spectra match with the Ia template. Follow-up observations were not complete due to the time limitation while SNe candidates would be observable. We are left with the candidates whose light curves indicate SNe Ia but were not spectroscopically confirmed. Our experience with the spectroscopically confirmed sample tells us that spectroscopic failure rate to confirm SNe Ia is only 10% of the light-curve selected candidates (Sako et al. 2008). This significant failure rate, however, applies to loosely selected candidates raised for spectroscopic follow-up that use light curves only in early days from the first detection, and it is substantially reduced for tightly light-curve selected SN Ia candidates, such as those used in this paper. A contamination of a few misidentified SNe Ia out of a hundred, if any, would not spoil global statistical analyses, such as those presented in this paper, beyond our statistical errors. Host galaxies of those candidates were spectroscopically observed later and their redshifts were measured. We refer to these cases as ‘host- z measured SNe Ia’. There are 168 objects in this category, which make our total sample to comprise 314 SNe Ia with known redshift.

For the supernova sample, g , r , and i -band light curves are measured by fitting images with a model of the galaxy background and the SN point spread function without pixel re-sampling frame by frame (scene-modeling photometry) (Holtzman et al. 2008). These SN multi-band photometric data are fit simultaneously by the SALT2 light curve fitter (Guy et al. 2007) to derive photometric parameters. Some SNe Ia in our sample are not suitable for detailed analysis: for SNe Ia discovered in the early or late phase of the observing season, i.e., early September and late November, light curves are observed only partially, with which it is often difficult to determine the accurate light curve shape and hence peak brightness. Some SNe Ia are faint and their signal-to-noise ratio at peak brightness is too low due to their large distances. We set the following criteria, as were done by Dilday et al. (2008), for the secure acquisition of light curves: (i) at least one measurement with $T_{\text{rest}} < -2$ days; (ii) at least one measurement with $T_{\text{rest}} > +10$ days; (iii) at least five measurements with $-20 < T_{\text{rest}} < +60$ days; (iv) at least one measurement with signal-to-noise ratio above 5 for each of g , r , and i ; (v) reasonable light curve fit whose reduced χ^2 calculated by SALT2 is less than 3 for probable and host- z SNe. For spectroscopically confirmed SNe Ia, the χ^2

criteria was not applied. Here T_{rest} is the rest-frame time from the epoch of peak brightness in the rest-frame B -passband. 222 SNe Ia among 314 passed these light curve criteria. The known peculiar SNe Ia, SN2005gj (Aldering et al. 2006; Prieto et al. 2007) and SN2005hk (Phillips et al. 2007) are rejected here. We limit the sky area to $-50.0 < \alpha < +55.0$ and $-1.25 < \delta < +1.25$ and the time coverage to 53626 (13 September 2005) $< t_{\text{max}}(\text{MJD}) < 53691$ (11 November 2005) to avoid the edge effects. This leaves 207 SNe Ia with us, the distribution of which is shown in Figure 1 as dotted histogram. We take this as the basic SN Ia sample. These selections, up to item (v), are readily implemented in the analysis procedure. The effective area of the survey is 262.5 square degree.

To make the sample incompleteness well defined for distant faint supernovae and the sample suitable to an application of the $1/V_{\text{max}}$ method to compute the LF, we make the sample magnitude limited. Figure 2 shows apparent maximum brightness in the r -passband as a function of redshift, which suggests us to set the limiting magnitude to be $r_{\text{lim}} = 21.5\text{mag}$. The figure shows that this ensures reasonable completeness of SNe Ia at $z = 0.20 - 0.25$. After applying this limiting magnitude, 137 SNe Ia are left with us for a magnitude limited sample, with the mean redshift $\langle z \rangle = 0.207$, which we take as our final sample for our analysis. Among magnitude limited sample, 72 are spectroscopically confirmed, 5 are spectroscopically probable and 60 are host- z SNe. Summary of the sample selection is shown in Table 1.

The solid histogram in Figure 1 represents the redshift distribution of this magnitude limited sample. The shade indicates the distribution expected for the empirical redshift distribution calculated using the code to generate light curves SNANA¹ (R. Kessler et al. 2009, private communication, submitted to PASP) assuming the SN Ia rate, $r_{\text{SNeIa}} \propto (1+z)^{1.5 \pm 0.6}$, which is inferred from the observed SDSS SNe Ia rate at low redshift (Dilday et al. 2008). The conditions of the SDSS observations, the software search efficiency and the light curve criteria are taken into account, and the normalisation is determined from the number of SNe below $z = 0.15$, for which redshift range SDSS SN observation is complete. The detail of simulation is described in Appendix. The shade stands for $\pm 20\%$ uncertainties of the normalization, corresponding to the Poisson error of the number of SNe Ia below $z = 0.15$. The SN frequency expected for no evolution of SN rate is shown by the dashed curve, which lies within the error indicated by shades. This figure shows that our sample is likely complete to $z < 0.20$.

The sample incompleteness at higher redshift is caused mainly by spectroscopic targetting and is given by fitting the ratio of observed number of SNe in our basic SN Ia sample to the simulated number as seen in Figure 3:

$$\epsilon(z) = \begin{cases} 1.0 & z \leq z_c \\ 1.0 - (z - z_c)/\Delta z & z_c < z < z_c + \Delta z \\ 0.0 & z \geq z_c + \Delta z, \end{cases} \quad (1)$$

¹<http://sdssdp47.fnal.gov/sdssn/SNANA-PUBLIC/>

where the best fit values are $z_c = 0.162 \pm 0.029$ and $\Delta z = 0.279 \pm 0.041$.

For each SN Ia the nearest primary object that resides within 10 arcsec from the SN is identified as its host galaxy in Catalog Archive Server of SDSS Data Release 6 (Adelman-McCarthy et al. 2008; see also Stoughton et al. 2002), with the identification visually confirmed. When misidentification is suspected, it arises mostly from deblended galaxies. Figure 4 shows the apparent r -band Petrosian magnitude distribution of host galaxies for 207 SNe Ia before the magnitude cutoff with the dotted histogram. The solid histogram is the host galaxies for our magnitude limit sample. There are 9 SNe whose host galaxies are not identified in the basic sample of 207 SNe (8 SNe in the 137 magnitude limit sample) within ~ 10 arcsec from a SN. These hostless SNe Ia are listed in Table 2, which gives the upper limit on absolute brightness of host galaxies searched in our survey to be $0.025 - 0.09L^*$ for the apparent magnitude limit of $r = 22.2$ mag. The physical distance corresponding to $10''$ is also given in the table. Petrosian magnitudes of u , g , r , i , and z -passband are used to compute rest-frame absolute brightness of host galaxies in 5 passbands using `kcorrect v4.1.4` (Blanton & Roweis 2007). Redshifts are fixed to the spectroscopic values.

3. Application of the $1/V_{\max}$ method

The light curves of SNe are fit by the SALT2 (Guy et al. 2007), which yields apparent maximum brightness in the rest-frame B -passband, m_B , together with the parameter describing the spectral variation x_1 and the optical depth representing the colour excess at maximum brightness c . The parameter x_1 is the weight of the next leading component of the spectral template and is related to the light curve shape parameter Δm_{15} (Phillips 1993), as $\Delta m_{15} = 1.09 - 0.161x_1 + 0.013x_1^2 + O(x_1^3)$ (Guy et al. 2007). SALT2 corrects for Galactic extinction following the extinction map of Schlegel et al. (1998).

We apply the $1/V_{\max}$ method to calculate LFs of SNe Ia (and of their host galaxies) to the magnitude limit sample of 137 SNe whose maximum brightness is brighter than 21.5 mag in the r -passband in the observed frame, by calculating the maximum redshift, z_{\max} , at which each SNe Ia (or their host galaxies) can be observed within the magnitude limit. Since the multicolour passband light curve fit by SALT2 gives us the spectral energy distribution of SN Ia, characterised with the shape parameter and the colour excess parameter, we can calculate expected apparent brightness in the r -passband in the observed frame at various redshifts using this spectral energy distribution. The limiting redshift gives the maximum volume that can be surveyed, V_{\max} , as

$$V_{\max}^i = \frac{\omega}{4\pi} \int_0^{z_{\max}^i} \frac{dV}{dz}(z) dz, \quad (2)$$

where ω is the solid angle $105 \times 2.5 = 262.5 \square^\circ$, and the index i refers to SNe Ia. Since V_{\max}^i is regarded as the volume surveyed to find i -th SNe, the LF is obtained by summing the inverse of V_{\max}^i within specified magnitude bins (ΔM) assuming that the LF is not evolving over the respective

redshift range. Taking into account the effect of visibility time and spectroscopic incompleteness, the LF is calculated as

$$\phi(M)\Delta M(\text{Mpc}^{-3}) = \sum_{i \in |M^i - M| < \Delta M/2} \frac{\tau}{V_{\text{max}}^i \times ct^i \times \epsilon(z^i)}, \quad (3)$$

where ct^i is the time of visibility in the rest-frame at which each SN Ia is observed. If the SN would be observed just at one epoch, as was done in a number of observations to derive the SN rate, the visibility time will be a time span over which each SNe can be detected above the detection limit: in this case a fainter SNe would have a shorter visibility time. In our case, however, observations have been made for the same field of sky continuously with the magnitude limit set for peak brightness. The visibility time will then be a time span of the survey observation. From the criteria on the date of maximum brightness, the visibility time in the observed frame is 65 days, and hence $ct^i = 65/(1 + z^i)$ days in the rest-frame. For SNe Ia M^i is absolute peak B -passband magnitude of SNe Ia, whose apparent rest-frame magnitude is estimated from SALT2. For host galaxies it is absolute magnitude in the rest-frame estimated using `kcorrect`. The factor $\epsilon(z)$ is the completeness correction, eq. (1). The LF is represented in units of per Mpc^3 , and τ (year) absorbs the time of the duration of observability when we deal with SNe. We take $\tau = 1$ yr as the unit. We describe in Appendix simulations we made to show that sample incompleteness and our corrections do not induce particular systematic errors to our analysis and our procedures allow us to recover the true LF, SN rate and related quantities.

4. Luminosity function of SNe Ia

To estimate the intrinsic brightness of SNe Ia, we must correct for dust extinction within host galaxies. In fact, SNe Ia show the variation in colour that could be attributed to dust extinction within host galaxies and/or interpreted as an intrinsic colour variation. The colour information is obtained from the colour excess parameter c of SALT2, which is defined by $c = (B - V)_{\text{max}} - \langle (B - V)_{\text{max}} \rangle$ at B -passband maximum brightness, where the second term is colour of the SN Ia templet. Figure 5 shows the distribution of this colour excess $c = E(B - V)$. The distribution is asymmetric with respect to $E(B - V) = 0$, similar to that of the SNLS sample (Astier et al. 2006). If we assume the color distribution as an exponential distribution $\propto \exp(-E(B - V)/\Delta)$ smeared by intrinsic Gaussian color distribution with the dispersion of σ , the observed distribution can be fitted with $\Delta = 0.048$ and $\sigma = 0.074$ as in Figure 5. This value of Δ is smaller than $\Delta = 0.138$ obtained for the nearby SN Ia sample by Jha et al. (2007). The mean and dispersion $\langle c \rangle = 0.176 \pm 0.280$ are compared with $\langle E(B - V) \rangle = 0.128 \pm 0.173$ from Jha et al. (2007). Several data points with high value of $E(B - V)$ greater than 0.5 contribute significantly to c . If they would be removed the mean and dispersion will become $\langle c \rangle = 0.061 \pm 0.107$. One may suspect that our sample may lack highly extinct or very red SNe due to selection effects. It is unlikely, however, that we dropped

such SNe at least at lower z where SNe are surveyed deep enough to reach brightness significantly fainter than are dimmed by extinction, unless $E(B - V) > 1$ which are dropped as our selection procedure for the SN Ia sample. The fact that the distribution does not change appreciably from low z to our redshift limit indicates that the decline of the event rate that give $E(B - V) > 0.2$ is not due to the selection effect and SNe that give a larger $E(B - V)$ is missing. The distribution of $E(B - V)$ corresponds, if interpreted as extinction, to extinction in the V passband ranging from -0.14 mag to 0.53 mag for one sigma, if $R_V = 3.1$ is assumed. The range of positive numbers is consistent with what is expected from extinction in the galactic discs with the HI column density $N_{\text{HI}} \lesssim 9 \times 10^{20} \text{ cm}^{-2}$ (Burstein & Heiles 1978), which is a typical value for disc galaxies unless they are edge-on. Extinction may also receive a contribution from SN itself and its environment. We come back to this problem in the end of the next section.

Figure 6 shows the distributions of A_V for the SNe Ia sample, taking the colour variation as reddening and assuming $R_V = 3.1$. Note that above $A_V = 3$ SNe Ia candidates, if any, are rejected during SN identification with light curves (Sako et al. 2008). This is compared with A_V for star forming field galaxies (dotted histogram), as calculated from the $\text{H}\alpha/\text{H}\beta$ Balmer line ratio obtained by SDSS within 3 arcsec of the central region of galaxies for $z < 0.2$ (Nakamura et al. 2004). The mean value of extinction of SNe Ia, $\langle A_V \rangle = 0.20$ mag, is significantly smaller than that for star forming field galaxies, $\langle A_V \rangle = 1.10$ mag. This suggests that most SNe Ia take place in regions clearer in dust than actively star forming regions.

We provisionally assume that the colour variation is due to extinction within host galaxies and that the extinction law is the same as that in our Galaxy with $R_V = 3.1$. We then estimate brightness of SNe Ia by correcting for extinction as $M_B - \beta \times c$ with $\beta = R_V + 1 = 4.1$. We note, however, that this ratio of total to selective extinction is not well justified. There are some indications that R_V for SNe Ia is lower than the Galactic value; Altavilla et al. (2004) used the bluest SNe Ia to estimate intrinsic colour of SN Ia and Reindl et al. (2005) used SNe Ia in early-type galaxies and far outlying SNe Ia in spiral galaxies. Both authors obtained $R_V \sim 2.5$. Nobili & Goobar (2008) also found a low value of $R_V = 1.75$ simultaneously deriving templates of SNe colour evolution in time and extinction. Astier et al. (2006) resulted in $R_V = 0.57$ and Kessler et al. (2009) gave $R_V = 2.18$. All R_V thus derived are smaller than the canonical value for the Milky Way.

Figure 7 shows the LF of SNe Ia in the B -passband, which is fitted with the Gaussian distribution with the mean and dispersion given in the upper left corner of each panel. The panel (a) assumes that the colour variation c arises from extinction with $\beta = 4.1$, giving the mean $M_B^0 = -19.42$ (in the Johnson zero point) and the dispersion 0.24 mag. If we would adopt a smaller value for R_V , the LF of SNe Ia becomes closer to a more regular Gaussian distribution with a smaller dispersion, as shown in Figure 7(b). The minimisation of dispersion with respect to β results in $\beta = 2.93$, which leads to the narrower Gaussian width of 0.16 mag with $M_B^0 = -19.32$, which is 0.10 mag fainter than with $\beta = 4.1$. Thus the smaller R_V gives more homogeneous SN Ia luminosity.

This small value of R_V obtained by minimizing the width of Gaussian fitted to SNe LF is an alternative manifestation of the low value of β obtained by Astier et al. (2006) by minimising the residual scatter in the Hubble diagram along with cosmological parameters. Kowalski et al. (2008) and Kessler et al. (2009) indicated that minimizing the scatter in the Hubble diagram tends to give R_V biased towards a value lower than the true value. Our simulation, however, shows that the value of β may be biased to the lower value but no more than by ~ 0.1 , so that this cannot be the reason for R_V being significantly smaller than 3.1. We do not conclude here that R_V is actually smaller but take $\beta = 4.1$ as our fiducial choice, keeping in mind the uncertainty from R_V in the analysis in what follows.

It has been argued that the maximum luminosity correlates with the light curve shape, or more specifically the decline rate (Δm_{15} , stretch, or SALT2’s x_1), and the inclusion of the correlation with it makes the behaviour of the LF tighter (Pskovskii 1984; Phillips 1993; Hamuy et al. 1996). We show in panels (c) and (d) of Figure 7 the LF where brightness is corrected by αx_1 , with α chosen to minimise the width of the Gaussian. In panel (c), β is fixed to our fiducial value of 4.1 and the minimisation gives $\alpha = 0.052$. In (d) both α and β are chosen to minimise the width, which results in $\beta = 2.52$ and $\alpha = 0.123$. The correlation of x_1 with brightness makes the Gaussian distribution narrower, especially for the case in which both α and β are optimised. The narrowest Gaussian is obtained with $\alpha = 0.123$ which corresponds to $\alpha' = 0.76$ where the correction for the light curve shape to brightness is expressed as $\alpha' \Delta m_{15}$. This value is consistent with 0.78 ± 0.18 obtained by Hamuy et al. (1996).

Figure 8 shows the correlation between brightness of SNe with the shape parameter and the colour excess. This correlation is the reason why the width of the luminosity function decreases upon inclusions of the light curve shape parameter and the colour excess parameter (with a small R_V). The correlation in the upper panel is represented by $M_B = -19.34 + 2.93c$ as shown in Figure 7(b), and that in the lower panel by $M_B - 4.1c = -19.43 - 0.052x_1$ as in Figure 7(c).

5. Host galaxies

The LFs of SNe Ia host galaxies, as calculated by the $1/V_{\max}$ method, are shown in Figures 9, 10 and 11 with solid histograms for the r , g , and i -passbands. Hostless SNe are indicated by shaded histogram at rightmost bin. We draw with solid curves the LF of general field galaxies obtained by Blanton et al. (2001), multiplied with the luminosity. The curves show good match of the LF of SN host galaxies with that of the field galaxies, which means that the LF of galaxies derived from SNe Ia faithfully represents that of galaxies in the field. We do not see any particular deviations between the two for three colour passbands g , r and i we studied, meaning that the occurrence of SNe Ia is primarily proportional to the luminosity of galaxies. Matching the two LF’s gives the SNe Ia rate in the conventional supernova unit (SNu), the SN rate per 10^{10} solar luminosity per

century r_L . Taking $M_r(\odot) = 4.62$, we obtain

$$r_L = 0.227 \pm 0.027 \text{ SNu}(r), \quad (4)$$

where we use the luminosity normalisation of Blanton et al. (2003) shifted to $z = 0.2$ using their evolution prescription with the Q parameter that represents the evolution of luminosity per redshift interval². This matching was done using data points at magnitude bins where the number of contributing galaxies are greater than 10 and error is Poisson from the SN number used in the $1/V_{\text{max}}$ analysis. The rate given above can be treated as a mean over the redshift range of our sample, the mean redshift $z = 0.20$. We may convert this rate expressed in SNu to the volumetric rate by multiplying the luminosity density. With reference to the luminosity density of Blanton et al. (2003), we find the volumetric rate of SNe Ia,

$$r_V = (3.63 \pm 0.43) \times 10^{-5} \text{ Mpc}^{-3} \text{ yr}^{-1}. \quad (5)$$

For g and i passbands the matching of the two LF's yield $r_L = 0.278 \pm 0.036 \text{ SNu}(g)$ and $r_L = 0.226 \pm 0.034 \text{ SNu}(i)$ taking $M_g(\odot) = 5.07$ and $M_i(\odot) = 4.52$ mag, respectively. These SN rates yield the volumetric rate $r_V = (3.86 \pm 0.50) \times 10^{-5} \text{ Mpc}^{-3} \text{ yr}^{-1}$ for the g passband and $r_V = (4.23 \pm 0.64) \times 10^{-5} \text{ Mpc}^{-3} \text{ yr}^{-1}$ for the i passband. The rates obtained from the three passbands agree with each other, within a 1σ error, showing the internal consistency. These SN rates agree with $r_V = (3.70 \pm 0.41 \pm 0.34) \times 10^{-5} \text{ Mpc}^{-3} \text{ yr}^{-1}$ obtained directly by summing up the LF of SNe Ia in Figure 7(a). Here the second error represents that arising from the completeness function given in eq. (1), which depends on the SN rate normalisation. If we take the B -band luminosity density $\mathcal{L}_B = 1.44 \times 10^8 L_{\odot}^B \text{ Mpc}^{-3}$ at $z = 0.2$, obtained by interpolating across five colours, we obtain the supernova rate per B -band luminosity

$$r_L = 0.257 \pm 0.028 \pm 0.024 \text{ SNu}(B). \quad (6)$$

This is compared with earlier measurements at low redshift compiled in Table 3.

Figure 12 shows that the SN rate per galaxy is proportional to luminosity of host galaxies, as one expects from the comparisons of the luminosity functions. The slope of the solid line is fixed to the rate at $0.227 \text{ SNu}(r)$ of Figures 9. The data point at the bottom left indicated with the open circle is for the ‘hostless SNe’ where the horizontal error bars indicate only the upper limit on host galaxy’s luminosity. We conclude that our hostless SNe Ia are consistent with them being occurred

² The normalisation of the luminosity functions of Blanton et al. (2003) differs significantly from Blanton et al. (2001) apart from the use of the different passbands defined at $z = 0.1$: the luminosity density of the latter is 20-40% larger than the former. The difference in the shape of the luminosity function, however, is modest and we adopt Schechter function parameters of Blanton et al. (2001) for the luminosity function in the g, r, i passbands at $z = 0$ by shifting only the normalisation. For the $g, r,$ and i passbands, we interpolated across the five colours at $z = 0.1$. The luminosity densities at $z = 0.2$ for the $g, r,$ and i passbands adopted are $\mathcal{L}_g = 1.39 \times 10^8 L_{\odot}/(\text{Mpc})^3$, $\mathcal{L}_r = 1.60 \times 10^8 L_{\odot}/(\text{Mpc})^3$, $\mathcal{L}_i = 1.87 \times 10^8 L_{\odot}/(\text{Mpc})^3$

in low luminosity galaxies beyond our detection limit but at the rate proportional to luminosity of host galaxies.

We present in Figure 13 the radial distance distribution of SNe Ia measured from the centre of host galaxies measured in the r -passband in physical distance units, where we do not correct for the projection effect caused by inclination of host galaxies. The relative distance between SN and the centre of host galaxy is measured within the accuracy of 0.1 arcsec, which corresponds to 0.4 kpc at $z = 0.3$ (Pier et al. 2003). The ordinate denotes numbers of the SN Ia per unit volume calculated by the formula similar to eq. (3). This radial distribution is well represented by the de Vaucouleurs profile with the half light radius of $r_e = 5.7$ kpc as drawn by the thin solid curve in Figure 13. We also draw the exponential profile (dotted curve) with the half light radius of $r_e = 3.6$ kpc, which falls off faster than the distribution of SNe Ia at an impact parameter larger than 10 kpc. The χ^2 of the best fit models, $\chi^2 = 8.2/11$ for the de Vaucouleurs profile and $\chi^2 = 11.7/11$ for the exponential profile, where fitting was done within 13 kpc using 13 data points, differ only a little but the difference is more apparent in the tail. When one uses the addition of the de Vaucouleurs and the exponential profiles, the best fit model shows bulge-to-disk luminosity ratio of 0.70, $r_e(\text{deV}) = 9.1$ kpc and $r_e(\text{exp}) = 2.4$ kpc with $\chi^2 = 5.0/9$. This fitted profile is drawn by thin dashed curve.

Our result does not agree with that of Bartunov et al. (2007) who claimed that SNe Ia in spiral galaxies are in a lower rate in the central part compared to SNe Ia in elliptical galaxies based on their supernova catalogue obtained by a compilation of SNe in the literature. Their earlier paper (Bartunov et al. 1992) claims that the radial dependence of surface density of SNe Ia can be expressed by the exponential profile. Our result does not agree with their conclusion, either.

The thick solid curve in Figure 13 shows the empirical mean r -passband light profile of field galaxies, which is constructed from the aperture flux of galaxies at $z = 0.025 - 0.030$ in Catalog Archive Server of SDSS Data Release 6 using values of `profMean`. The innermost bin may be somewhat affected by finite size seeing. The normalisation is set to the same as Figure 9 while taking into account the luminosity evolution of galaxies from $z = 0.025 - 0.030$ to $z = 0.2$ using the Q parameter of Blanton et al. (2003) while fixing the shape of the light profile. The light profile of galaxies is consistent with the exponential disc plus de Vaucouleurs spheroid model with the bulge-to-disk luminosity ratio of 0.56. We note that the radial distribution of SNe Ia, at least for the bulk of SNe, is consistent with the light distribution ($\chi^2 = 11.2/13$), except for that at a large distance beyond 10 kpc where we see some excess occurrence of SNe. It is interesting to see that some SNe Ia occur at a large distance where the galaxy contributes little light: at > 10 kpc we expect from the global rate, $1.31 \times 10^{-5} \text{ Mpc}^{-3}\text{yr}^{-1}$ SNe Ia with the light distribution of the de Vaucouleurs profile and $0.15 \times 10^{-5} \text{ Mpc}^{-3}\text{yr}^{-1}$ SNe Ia with the exponential profile, which are compared with observed $0.55 \times 10^{-5} \text{ Mpc}^{-3}\text{yr}^{-1}$ SNe Ia. The radial distribution of SNe Ia also supports the proposition that the occurrence of SNe Ia is primarily proportional to the luminosity of host galaxies.

We study the dependence of the SN rate on colour of host galaxies, to examine whether the occurrence of SNe Ia would correlate with the star formation activity. In Figure 14 the histogram represents the SN host galaxies and the solid curve shows the luminosity weighted colour function of field galaxies which is calculated using bivariate function $\phi(M_r, g - r)$ (Blanton et al. 2001), as

$$\Phi_L(g - r)d(g - r) = \int_{-24.25}^{-14.75} dM_r \phi(M_r, g - r) \times 10^{0.4(M_{\odot,r} - M_r)} d(g - r), \quad (7)$$

where $\phi(M_r, g - r)$ is evaluated for $-24.25 < M_r < -14.75$ and $0.12 < g - r < 0.88$ on the 20×20 grid. The abscissa is rest-frame colour after the K-correction. The normalisation is taken to be the same as that in Figure 9. Morphological types of galaxies are indicated with the corresponding colours according to Fukugita et al. (2007) with the error bar representing the dispersion of colours in the morphologically classified sample. This figure shows that the colour distribution of SNe Ia host galaxies traces well that of field galaxies, and we do not see any particular excess of SNe Ia host galaxies for bluer, late type or irregular galaxies, beyond one sigma level. In this comparison we do not take into account the evolution of galaxy colour to $z = 0.2$.

In particular we may be interested in the difference of the SN rate between the elliptical galaxies and other galaxies. If we select galaxies with colour $0.73 < g - r < 0.81$ corresponding to elliptical galaxies (with contaminations from S0 and some Sa galaxies) we obtain the SN rate 0.194 ± 0.062 SNu(r) which is compared with 0.255 ± 0.035 for galaxies with $g - r < 0.73$ (Sa galaxies or later). We observe a $31 \pm 35\%$ enhancement in the SN rate relative to galaxy luminosity in late type galaxies compared to that in elliptical galaxies, though the effect is only at one sigma. We do not see a particular enhancement of SN rate per luminosity, however, among late type galaxies, where the star formation rate increases towards later type morphologies (Nakamura et al. 2004).

$u - g$ colour is more sensitive to the star formation activity than $g - r$, but u -band brightness is too faint to us for most host galaxies: SN host galaxies brighter than 21 mag are less than 40% for our magnitude limit supernova sample, and we are not able to draw a meaningful conclusion from the $u - g$ colour distribution. The SN host galaxies are also too faint for SDSS spectroscopy (Strauss et al. 2002), and we cannot estimate the star formation rate directly, unless we resort to population synthesis colours, which are not well constrained without u colour. Therefore, we do not find clear evidence that points to the correlation of the SN rate with the star formation activity.

Mannucci et al. (2005) and Sullivan et al. (2006) give models of SN Ia rates with the two components of progenitors, one explosions of old binary stars with a large delay time from the formation and the other explosions with a short delay time after the system formed. Mannucci et al. (2005) give SNe Ia rate that depends on the morphological type of host galaxies in units of SNu(K). We may use their rate to estimate the number of SNe Ia for each morphological type using morphological-type dependent luminosity density of field galaxies, as given by Nakamura et al. (2003) with the aid of the conversion from the r to the K -passband (Nagamine et al. 2006). This model gives $r_V = 3.0 \times 10^{-5} \text{ Mpc}^{-3} \text{ yr}^{-1}$, where 31% are the prompt component, which is consistent with the difference in SN Ia rate relative to galaxy luminosity between elliptical galaxies and

spiral galaxies. The total rate also agrees with our rate in equation (5). The detailed numbers are presented in Table 4.

Sullivan et al. (2006) modelled SN Ia rate as a function of stellar masses and mean SFRs of host galaxies. We use the morphology dependent luminosity density of Nakamura et al. (2003) and the morphologically dependent star formation rate calculated from the star formation rate of the bulge and disk components given in Nagamine et al. (2006). The predicted SN Ia rate is $r_V = 2.6 \times 10^{-5} \text{ Mpc}^{-3} \text{ yr}^{-1}$, of which 13% are prompt: see also Table 4. The predicted numbers of SNe Ia are plotted in Figure 14 as dotted (Mannucci et al.’s model) and dashed (Sullivan et al.’s model) curves taking the colour distribution of each morphological type as a Gaussian with mean and dispersion given by Fukugita et al. (2007). The χ^2 for the two models are 15.1 and 23.6 for 11 degrees of freedom using data for $0.1 < g - r < 1.0$.

The currently available two component models are marginal to represent our data, but are consistent with the observed number of SNe Ia, as shown by the histogram in Figure 14 allowing for large uncertainties. The prompt component is rather minor and not very manifest in the integrated rates for low z SNe, as in our analysis. The model prediction for Im galaxies is low, which is due to the low luminosity density of Im galaxies in the SDSS morphologically classified sample. In Nakamura et al. (2003) Im galaxies contribute only $\sim 1\%$ of the total luminosity density, which may be due to the selection effect that disfavours Im galaxies. This contrasts to the indication from the colour function of Blanton et al. (2001), which suggests that galaxies bluer than $(g - r) < 0.42$ contribute by $\sim 15\%$ of total luminosity. If the luminosity density of Im galaxies is this large, however, the number of SNe Ia in Im galaxies would be 10 times more that would largely overshoot our observed numbers of SNe. To identify the prompt component and test the two component hypothesis, we need a sample where the prompt component is dominant, or the sample with which both star formation rate and SN rate can more accurately be measured.

Our sample allows us to study if the properties of SNe Ia would depend on the property of host galaxies. It has occasionally been claimed that bright SNe Ia appear more often in late type galaxies, while SNe Ia in early type galaxies are subluminous (Filippenko 1989; della Valle & Panagia 1992; Reindl et al. 2005; Sullivan et al. 2006). This has been counted as one of the reasons that SN Ia calibration of nearby galaxy’s distance led to a smaller value of the Hubble constant in the past. Figure 15(a) plots the maximum brightness of SNe Ia in our sample as a function of $g - r$ colour of host galaxies: mean brightness of SNe Ia does not change across colours of galaxies from E to Im. In particular the plot does not indicate any evidence that SNe Ia in bluer galaxies are systematically brighter or those in red galaxies are fainter. Both mean and dispersion of luminosity are nearly constant with respect to galaxy colour as seen in the figure.

Figure 15(b) shows the plot of the x_1 parameter, which represents the decline rate of SNe Ia brightness, against $g - r$ colour of host galaxies. The upper values of x_1 does not change with respect to colour from E to Im galaxies, but the lower value shows the trend that it decreases from -0.5 (or $\Delta m_{15} \simeq 1.2$) for Im galaxies to -3 ($\Delta m_{15} \simeq 1.7$) for E and S0 galaxies. It is noted that

large negative values of x_1 are seen only in early-type galaxies. This causes some dependence of x_1 on colour of host galaxies as seen in the figure. The slope, however, is small enough to cause any effect on brightness of SNe Ia through the correction of $0.12x_1$.

Similarly Figure 16 shows maximum brightness of SNe Ia on luminosity of host galaxies, showing that the former does not depend on luminosity of the host. Note that we expect that average metallicity of the host galaxy changes by 0.59 dex in this luminosity range (Tremonti et al. 2004). The x_1 parameter changes slightly as luminosity of host galaxies changes.

We also examine the dependence of the c parameter and the x_1 parameter on the distance from the centre of galaxies as shown in Figure 17. The colour excess $c = E(B - V)$ stays nearly at ≈ 0.08 with the dispersion of 0.07 and does not show a systematic change from 1 kpc to 15 kpc. In particular, we observe that the colour excess does not decrease as we go farther away from the centre of galaxies, where stars, and hence dust, are expected to decrease. The trend we see here does not change if we limit the SNe to $z < 0.2$ with which SNe Ia that would receive reasonably large extinction are included in the sample. This finding suggests us to interpret that the observed reddening is mostly associated with individual supernovae, either extinction from supernova itself and/or circum-supernova dust or intrinsic colour variation of the supernova, rather than interstellar dust in host galaxies. This would also give us an upper limit on the model as to the amount of dust produced around SNe Ia. We observe only 7 SNe Ia which shows colour excess more than $E(B - V) \geq 0.3$ mag among our 137 SN Ia sample. In addition, we do not observe a systematic dependence of the x_1 parameter on the distance from the centre of galaxies; see Figure 17(b).

6. Conclusion

The SNe Ia sample acquired in the SDSS II, containing 137 low redshift SNe from $z = 0.05$ to 0.3, indicates that the occurrence of SNe Ia is primarily proportional to luminosity of galaxies. The LF of SN Ia host galaxies matches very well with that of field galaxies multiplied by luminosity, and colour of SN Ia host galaxies does not differ from that of field galaxies. Our low redshift sample does not indicate an active signature that the occurrence of SNe Ia follows star formation activity, except that possible enhancement in the SN Ia rate is noted in late type galaxies ($\lesssim 31 \pm 35\%$) compared with the rate in elliptical galaxies. Our low redshift sample is compatible with the two component model where the effect of the prompt component is modest (10–30% of the total rate), as in the current models. We are not able to differentiate SN rates among late type galaxies. Our sample contains 8 SNe Ia, whose host galaxies were not identified. It is shown, however, that they are consistent with them occurred in low luminous galaxies beyond the survey limit for galaxies. Luminosity of SNe Ia does not appear to depend upon luminosity or colour of host galaxies.

The luminosity function of SNe Ia is Gaussian with $M_B = -19.42$ and $\sigma = 0.24$ mag (FWHM is a factor 1.4 in luminosity), if the colour variation is interpreted as reddening obeying the extinction law of the Milky Way with the standard value $R_V = 3.1$. This Gaussian distribution is further

tightened and $\sigma = 0.14$ mag if the extinction to reddening ratio R_V is reduced to ≈ 2 and if the correlation is taken into account between maximum brightness and the decline rate. Reddening of SN Ia, inferred from the colour variation, is 0.1 mag in A_V , which is lower approximately by a factor of 5 than that for star forming field galaxies measured from $H\alpha$ and $H\beta$ emission.

We also showed that the distribution of the SN Ia occurrence, that extends to a few tens of kpc, agrees with the general light distribution of galaxies that have bulges with the de Vaucouleurs type profiles. The variation of colours of SN Ia is constant and does not depend on the distance from the centre of galaxies unlike what is expected for the supernova that would happen in the galactic disc. The colour variation of SNe Ia may likely be ascribed to intrinsic colour variation or immediate neighbourhood of supernovae rather than extinction in host galaxies. The total column density of dust should not give extinction more than 0.2 mag in the V passband.

We should like to thank the review group of the SDSS-II Supernova Survey Project (Josh Frieman, Bob Nichol, Saurabh Jha, Benjamin Dilday) and Don Schneider and Richard Kessler for reviewing the manuscript and useful comments improving the manuscript. NY acknowledges support by the JSPS core-to-core program “International Research Network for Dark Energy” and the JSPS-USA bilateral programme, MF is supported by Grant-in-Aid of the Ministry of Education in Japan, and Ambrose Monell Foundation at Princeton.

Funding for the SDSS and SDSS-II has been provided by the Alfred P. Sloan Foundation, the Participating Institutions, the National Science Foundation, the U.S. Department of Energy, the National Aeronautics and Space Administration, the Japanese Monbukagakusho, the Max Planck Society, and the Higher Education Funding Council for England. The SDSS Web Site is <http://www.sdss.org/>.

The SDSS is managed by the Astrophysical Research Consortium for the Participating Institutions. The Participating Institutions are the American Museum of Natural History, Astrophysical Institute Potsdam, University of Basel, University of Cambridge, Case Western Reserve University, University of Chicago, Drexel University, Fermilab, the Institute for Advanced Study, the Japan Participation Group, Johns Hopkins University, the Joint Institute for Nuclear Astrophysics, the Kavli Institute for Particle Astrophysics and Cosmology, the Korean Scientist Group, the Chinese Academy of Sciences (LAMOST), Los Alamos National Laboratory, the Max-Planck-Institute for Astronomy (MPIA), the Max-Planck-Institute for Astrophysics (MPA), New Mexico State University, Ohio State University, University of Pittsburgh, University of Portsmouth, Princeton University, the United States Naval Observatory, and the University of Washington.

A. Verification of the analysis method

In order to examine the validity of our analysis, we have made simulations for our observation creating a set of light curves using SALT2 model in combination with SNANA. The distribution of

x_1 parameter is assumed to be a Gaussian with the mean 0 and the dispersion 0.90. The distribution of c is a Gaussian with the mean 0.063 and the dispersion 0.11. We assume the relation involving absolute magnitude M , x_1 and c ,

$$M = M_0 - \alpha x_1 + \beta c \tag{A1}$$

with $\alpha = 0.10$ and $\beta = 2.45$. The intrinsic dispersion of 0.11 mag was applied for every passbands and every epochs. The epochs of observation is fixed to actual date and the signal to noise ratio of each observing point was calculated by using real observational condition of our observation including seeing and sky brightness. The detection efficiency searching for variable objects is also included in our simulation, and the SN Ia rate of $r_{\text{SNeIa}} = 2.2 \times 10^{-5} (1+z)^{1.5}$ ($\text{Mpc}^{-3} \text{yr}^{-1}$) is assumed. The cut based on the quality of light curves as described in the text is also applied to the simulation, and the spectroscopic incompleteness of eq. (1) is applied with $z_c = 0.15$ and $\Delta z = 0.3$. The simulation generated 210 SNe light curves. We make 50 sets of simulated light curves and applied the method the same as that to the observed dataset. The incompleteness correction $\epsilon(z)$ in eq. (3) is calculated separately for each simulation set.

Figure 18 shows the comparison of the input and the output SN LF after correcting for the effect of c parameter. Solid curve represents the expected LF taking into account the error of the determination of m_B and c from light curve fits. Histograms and error bars are the mean and dispersion in each magnitude bin calculated from the 50 simulated light curve sets. A good agreement is seen between solid curves and histograms.

We also make a simulation incorporating the completeness as a function of apparent peak r -passband brightness of SNe like $\epsilon(m) = 1.0 - (r_{\text{max}} - 19.75)/3.15$ to see the effect when the completeness is not a function of redshift but of apparent peak magnitude. The completeness $\epsilon(z)$ in eq. (3) is estimated as a function of redshift. The result is shown in Fig. 19. We see again a good agreement between the input and output SNe. This is due to the fact that redshift and apparent peak magnitude are well correlated.

Good agreements are seen between input and output SN LF's for both cases where incompleteness is a function of redshift and of apparent peak r -passband magnitude. The analysis adopted in this paper does not suffer from particular systematic effects while dealing with apparently a dataset with sample incompleteness. The volumetric SN rate is recovered to be $(2.95 \pm 0.42) \times 10^{-5}$ and $(3.04 \pm 0.51) \times 10^{-5}$ depending on whether incompleteness is taken to be a function of redshift or apparent magnitude, respectively. These numbers are compared with the input value of 3.18×10^{-5} ($\text{Mpc}^{-3} \text{yr}^{-1}$). The volumetric SN rate is properly recovered within the error.

We also examine the distribution of the c and x_1 parameters of SALT2 light curve fit in Fig. 20. SNe with high c value or low x_1 value will be faint and such SNe may suffer from incompleteness. The analysis is similar to that of the LF. In eq. 3, we replace absolute magnitude M with the colour parameter c or the shape parameter x_1 . We do not see any systematic effect for the recovered distribution. We change the assumed distributions of the c and x_1 parameters and the relation among M , x_1 and c in a way they are consistent with the observed SNe, and

calculate the completeness of the observed sample. This procedure is iterated till the convergence (one or two iterations are sufficient). The final values are $x_1 = 0 \pm 0.96$, $c = 0.039 \pm 0.093$ and $M = M_0 - 0.12x_1 + 2.52c$, where the last relation agrees with the one obtained by minimising the width of the LF of SNe Ia as seen in Fig. 7(d). With these procedures the redshift distribution of the observed SNe is reproduced as shown in Figure 21.

We conclude that the method we used in this paper works well even for the data with incompleteness after the proper account taken for incompleteness. We do not expect any specific biases in the analysis.

REFERENCES

- Adelman-McCarthy, J. K., et al. 2008, *ApJS*, 175, 297
- Aldering, G., et al. 2006, *ApJ*, 650, 510
- Altavilla, G., et al. 2004, *MNRAS*, 349, 1344
- Astier, P., et al. 2006, *A&A*, 447, 31
- Barbon, R., Cappellaro, E., & Turatto, M. 1989, *A&AS*, 81, 421
- Bartunov, O. S., Makarova, I. N., & Tsvetkov, D. I. 1992, *A&A*, 264, 428
- Bartunov, O. S., Tsvetkov, D. Y., & Pavlyuk, N. N. 2007, *Highlights of Astronomy*, 14, 316
- Blanc, G., et al. 2004, *A&A*, 423, 881
- Blanton, M. R., et al. 2001, *AJ*, 121, 2358
- Blanton, M. R., et al. 2003, *ApJ*, 592, 819
- Blanton, M. R., & Roweis, S. 2007, *AJ*, 133, 734
- Botticella, M. T., et al. 2008, *A&A*, 479, 49
- Burstein, D., & Heiles, C. 1978, *ApJ*, 225, 40
- Cappellaro, E., Evans, R., & Turatto, M. 1999, *A&A*, 351, 459
- Dahlen, T., Strolger, L.-G., & Riess, A. G. 2008, *ApJ*, 681, 462
- Dallaporta, N. 1973, *A&A*, 29, 393
- della Valle, M., & Panagia, N. 1992, *AJ*, 104, 696
- Dilday, B., et al. 2008, *ApJ*, 682, 262

- Filippenko, A. V. 1989, PASP, 101, 588
- Frieman, J. A., et al. 2008, AJ, 135, 338
- Fukugita, M., Ichikawa, T., Gunn, J. E., Doi, M., Shimasaku, K., & Schneider, D. P. 1996, AJ, 111, 1748
- Fukugita, M., et al. 2007, AJ, 134, 579
- Gunn, J. E., et al. 1998, AJ, 116, 3040
- Gunn, J. E., et al. 2006, AJ, 131, 2332
- Guy, J., et al. 2007, A&A, 466, 11
- Hamuy, M., Phillips, M. M., Suntzeff, N. B., Schommer, R. A., Maza, J., & Aviles, R. 1996, AJ, 112, 2391
- Hardin, D., et al. 2000, A&A, 362, 419
- Hogg, D. W., Finkbeiner, D. P., Schlegel, D. J., & Gunn, J. E. 2001, AJ, 122, 2129
- Holtzman, J. A., et al. 2008, AJ, 136, 2306
- Ivezić, Ž., et al. 2004, Astronomische Nachrichten, 325, 583
- Jha, S., Riess, A. G., & Kirshner, R. P. 2007, ApJ, 659, 122
- Kowalski, M. et al. 2008, ApJ, 686, 749
- Kessler, R., et al. 2009, submitted to ApJS
- Madgwick, D. S., Hewett, P. C., Mortlock, D. J., & Wang, L. 2003, ApJ, 599, L33
- Mannucci, F., Della Valle, M., Panagia, N., Cappellaro, E., Cresci, G., Maiolino, R., Petrosian, A., & Turatto, M. 2005, A&A, 433, 807
- Miller, D., & Branch, D. 1990, AJ, 100, 530
- Nagamine, K., Ostriker, J. P., Fukugita, M., & Cen, R. 2006, ApJ, 653, 881
- Nakamura, O., Fukugita, M., Yasuda, N., Loveday, J., Brinkmann, J., Schneider, D. P., Shimasaku, K., & SubbaRao, M. 2003, AJ, 125, 1682
- Nakamura, O., Fukugita, M., Brinkmann, J., & Schneider, D. P. 2004, AJ, 127, 2511
- Nobili, S., & Goobar, A. 2008, A&A, 487, 19
- Phillips, M. M. 1993, ApJ, 413, L105

- Phillips, M. M., et al. 1999, *AJ*, 118, 1766
- Phillips, M. M., et al. 2007, *PASP*, 119, 360
- Pier, J. R., Munn, J. A., Hindsley, R. B., Hennessy, G. S., Kent, S. M., Lupton, R. H., & Ivezić, Ž. 2003, *AJ*, 125, 1559
- Poznanski, D., et al. 2007, *MNRAS*, 382, 1169
- Prieto, J. L., et al. 2007, *ArXiv e-prints*, 706, arXiv:0706.4088
- Pskovskii, Y. P. 1984, *Soviet Astronomy*, 28, 658
- Reindl, B., Tammann, G. A., Sandage, A., & Saha, A. 2005, *ApJ*, 624, 532
- Richardson, D., et al. 2002, *AJ*, 123, 745
- Sako, M., et al. 2008, *AJ*, 135, 348
- Schlegel, D. J., Finkbeiner, D. P., & Davis, M. 1998, *ApJ*, 500, 525
- Smith, J. A., et al. 2002, *AJ*, 123, 2121
- Stoughton, C., et al. 2002, *AJ*, 123, 485
- Strauss, M. A., et al. 2002, *AJ*, 124, 1810
- Sullivan, M., et al. 2006, *ApJ*, 648, 868
- Tammann, G. A. 1982, *NATO ASIC Proc. 90: Supernovae: A Survey of Current Research*, ed. by M. J. Rees and R.-J. Stoneham, 371
- Tremonti, C. A., et al. 2004, *ApJ*, 613, 898
- York, D. G., et al. 2000, *AJ*, 120, 1579
- Zheng, C., et al. 2008, *AJ*, 135, 1766

Table 1. Sample selection summary

Criteria	Number
total	314
spectroscopic/confm'd	130
spectroscopic/probable	16
light curve selection	168
secure light curve	222
good sky area & date	207
$r_{\text{lim}} < 21.5$	137
no host galaxies	8

Table 2. Hostless SNe Ia

SDSS ID	IAU Name	Redshift	Luminosity Limit (L_r^*)	Dist. of $10''$ (kpc)
2943	2005go	0.2659	0.055	40.7
5994	2005ht	0.1885	0.025	31.2
6780	2005iz	0.2046	0.029	33.1
6924	2005ja	0.3286	0.089	47.2
6933	2005jc	0.2137	0.033	34.5
7475	2005jn	0.3188	0.085	46.7
7335	2005kn	0.1975	0.028	32.6
3565		0.2885	0.067	43.4
8030 ^a	2005jv	0.4226	0.161	55.5

^aOutside the magnitude limited sample

Table 3. SNe Ia Rate Measurements

Reference	Redshift	Rate (SNU)
Cappellaro et al. (1999)	0	0.18 ± 0.05
Dilday et al. (2008) ^a	0.09	$0.246^{+0.076}_{-0.060}$
Madgwick et al. (2003)	0.098	0.196 ± 0.098
Blanc et al. (2004)	0.13	$0.125^{+0.044+0.028}_{-0.034-0.028}$
Hardin et al. (2000)	0.14	$0.22^{+0.17+0.06}_{-0.10-0.03}$
This work	0.20	$0.257 \pm 0.028 \pm 0.024$
Botticella et al. (2008)	0.3	$0.22^{+0.10+0.16}_{-0.08-0.14}$

^a B -band luminosity density of $j_B = 1.19 \times 10^8 L_{\odot}^B \text{ Mpc}^{-3}$ was used to convert from the value per comoving volume unit.

Table 4. Predicted SNe Ia rate in the two component model

morph. type	$g - r$	j_r $10^8 L_r(\odot) \text{Mpc}^{-3}$	L_K/L_r	Mannucci et al. model			Sullivan et al. model		
				N_A (delayed) $10^{-5} \text{Mpc}^{-3} \text{yr}^{-1}$	N_B (prompt) $10^{-5} \text{Mpc}^{-3} \text{yr}^{-1}$	$N_A + N_B$ $10^{-5} \text{Mpc}^{-3} \text{yr}^{-1}$	N_A (delayed) $10^{-5} \text{Mpc}^{-3} \text{yr}^{-1}$	N_B (prompt) $10^{-5} \text{Mpc}^{-3} \text{yr}^{-1}$	$N_A + N_B$ $10^{-5} \text{Mpc}^{-3} \text{yr}^{-1}$
E,S0	0.75	0.62	3.32	0.720	0.000	0.720	0.882	0.052	0.935
S0/a-Sb	0.64	1.00	2.77	0.970	0.304	1.274	1.052	0.189	1.240
Sbc-Sd	0.51	0.37	2.52	0.326	0.495	0.821	0.326	0.088	0.414
Im	0.36	0.02	2.15	0.015	0.127	0.142	0.013	0.006	0.019
Total		2.01		2.031	0.926	2.957	2.273	0.335	2.608

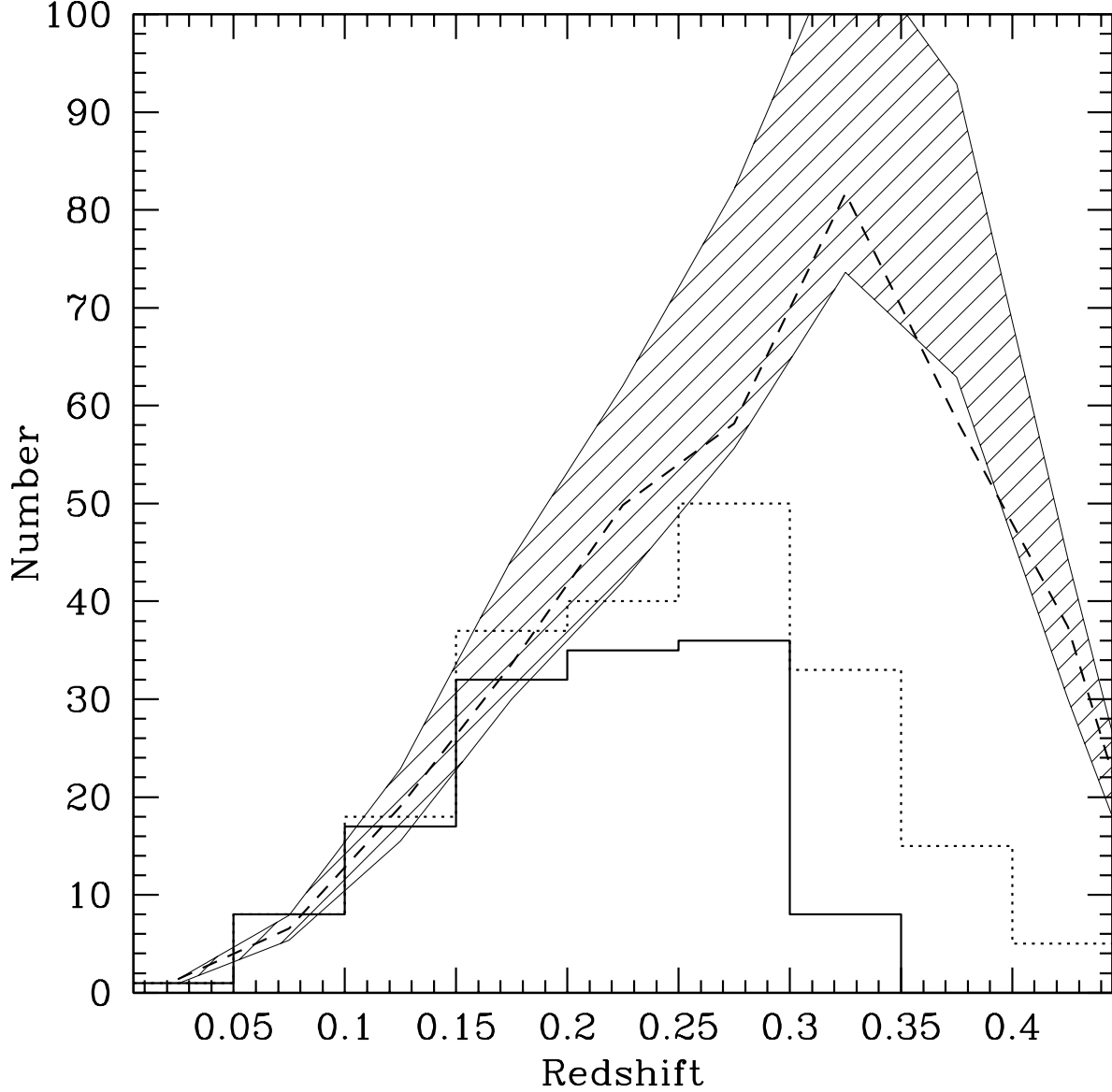


Fig. 1.— Redshift distribution of our samples. The dotted histogram represents the basic sample comprising 207 SNe Ia. The solid histogram is the magnitude limited sample, our final sample, comprising 137 SNe Ia with $r_{\max} < 21.5$ mag used to derive the LF. Shaded region shows the expected distribution when SNe Ia are distributed as $\propto (1+z)^{1.5}$ with the selection criteria we adopted taken into account. Shading stands for 20% uncertainty in the normalization. Dashed curve is the expected distribution when SNe Ia rate shows no evolution in z .

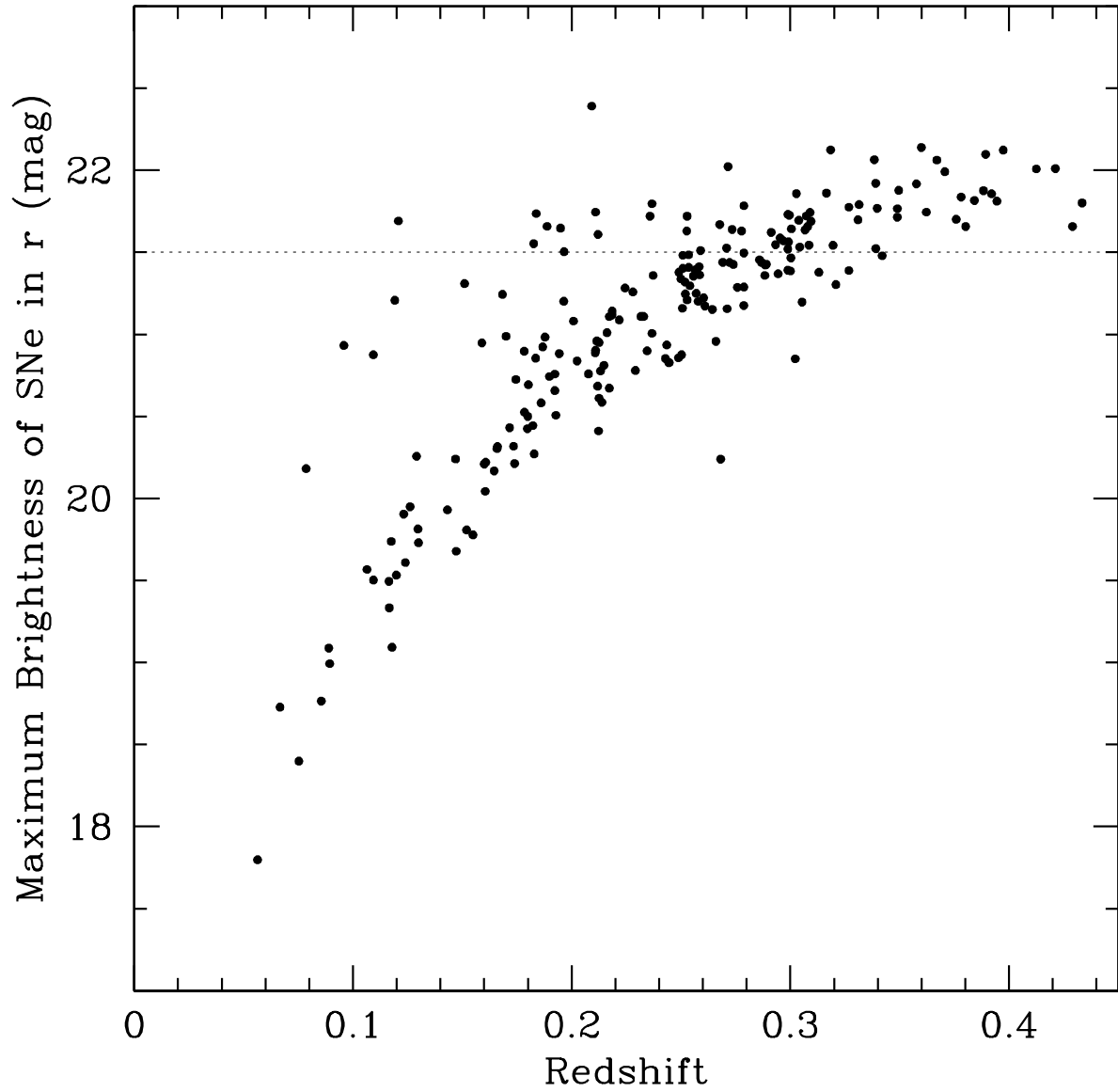


Fig. 2.— Apparent maximum brightness of 207 SNe Ia in the r -band as a function of redshift. Horizontal dotted line denotes the magnitude limit of $r_{lim} = 21.5$ mag. Brightness is not corrected for extinction or colour excess.

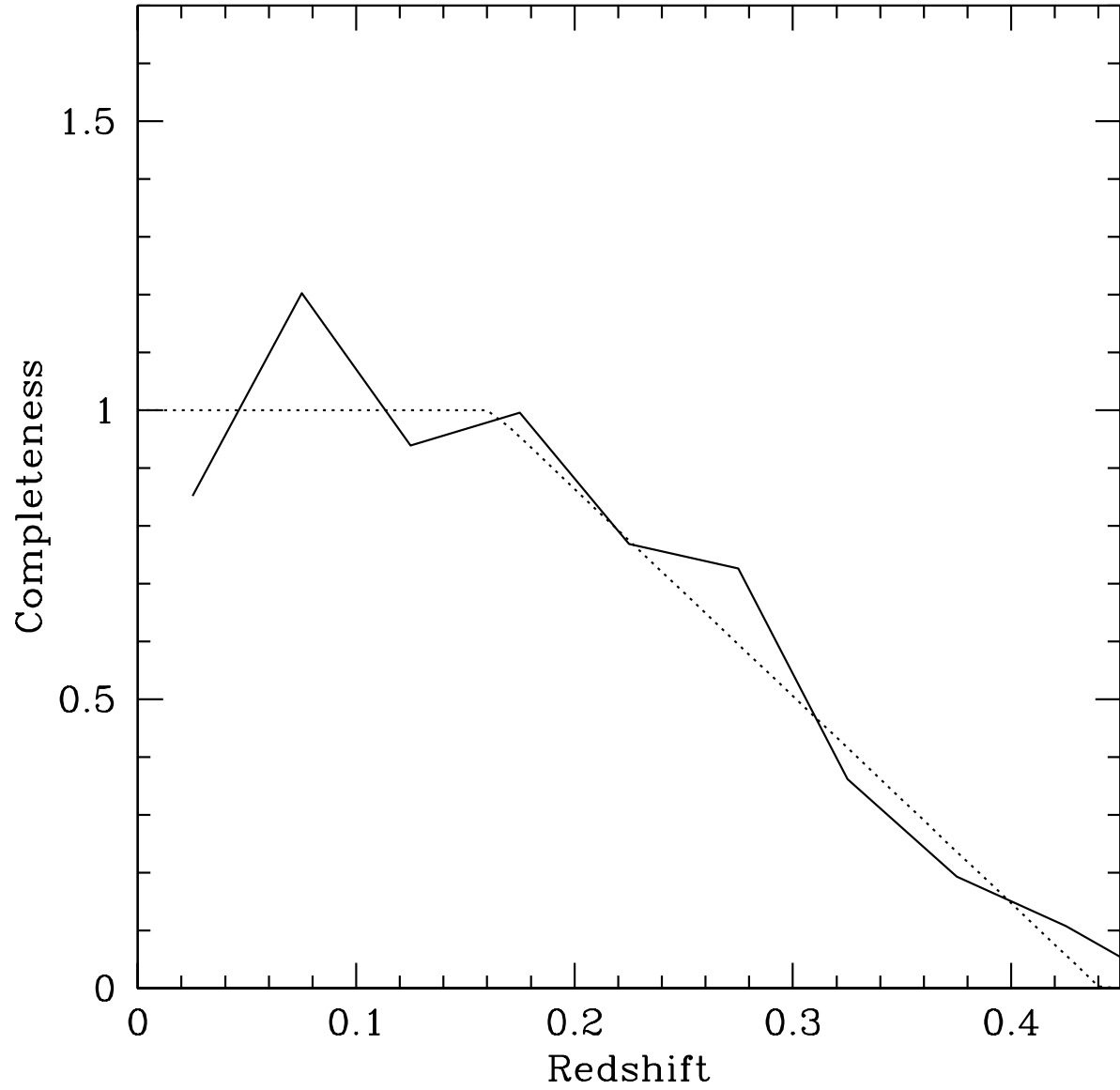


Fig. 3.— Solid line shows the ratio of the number of SNe Ia in our basic sample to the simulation as a function of redshift. Dotted line shows the completeness function eq.(1) used in this paper.

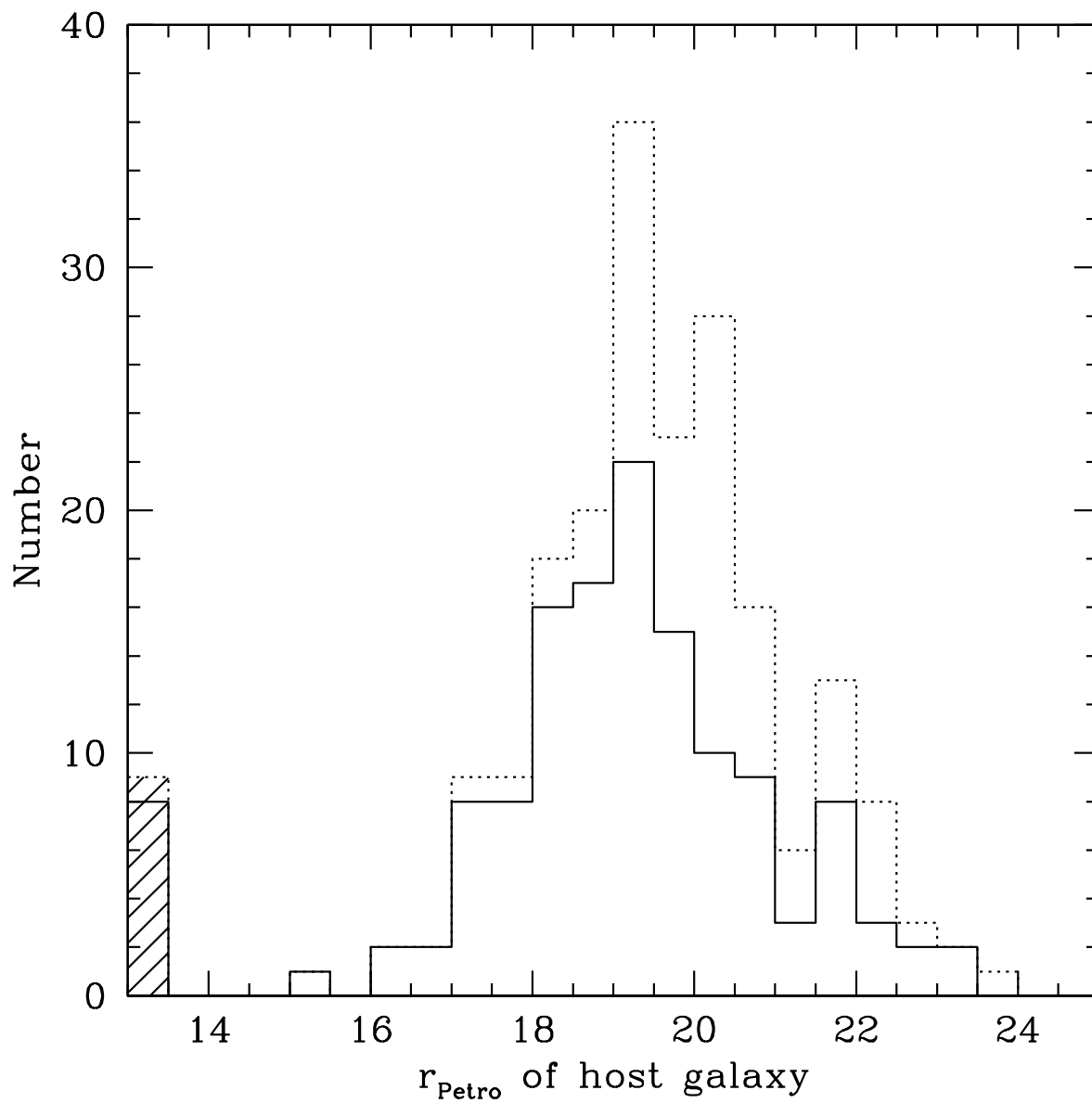


Fig. 4.— Distributions of apparent r -band Petrosian magnitude of host galaxies of our basic SN Ia sample (dotted histogram) and of the magnitude limited sample (solid histogram). There are 9 (or 8) SNe Ia whose host galaxies are not identified in the two samples, which are indicated in the leftmost bin with shades.

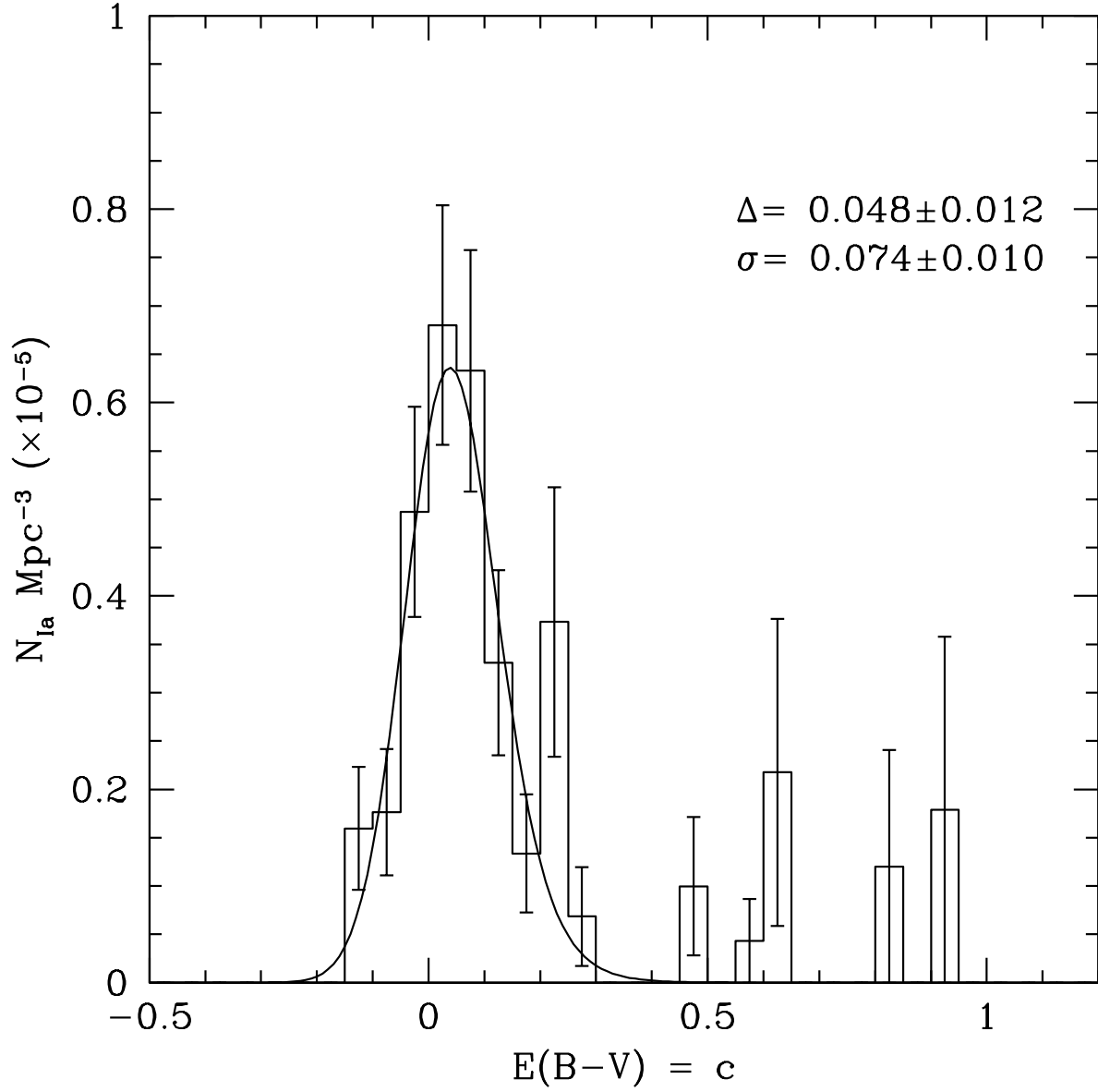


Fig. 5.— Distribution of colour excess $E(B-V) = c$ calculated from the magnitude limited sample. The curve is the Gaussian with the function $p(E(B-V)) \propto \exp(-E(B-V)/\Delta)$ for $E(B-V) > 0$ and $p(E(B-V)) = 0.0$ for $E(B-V) < 0$ convolved with Gaussian (see text).

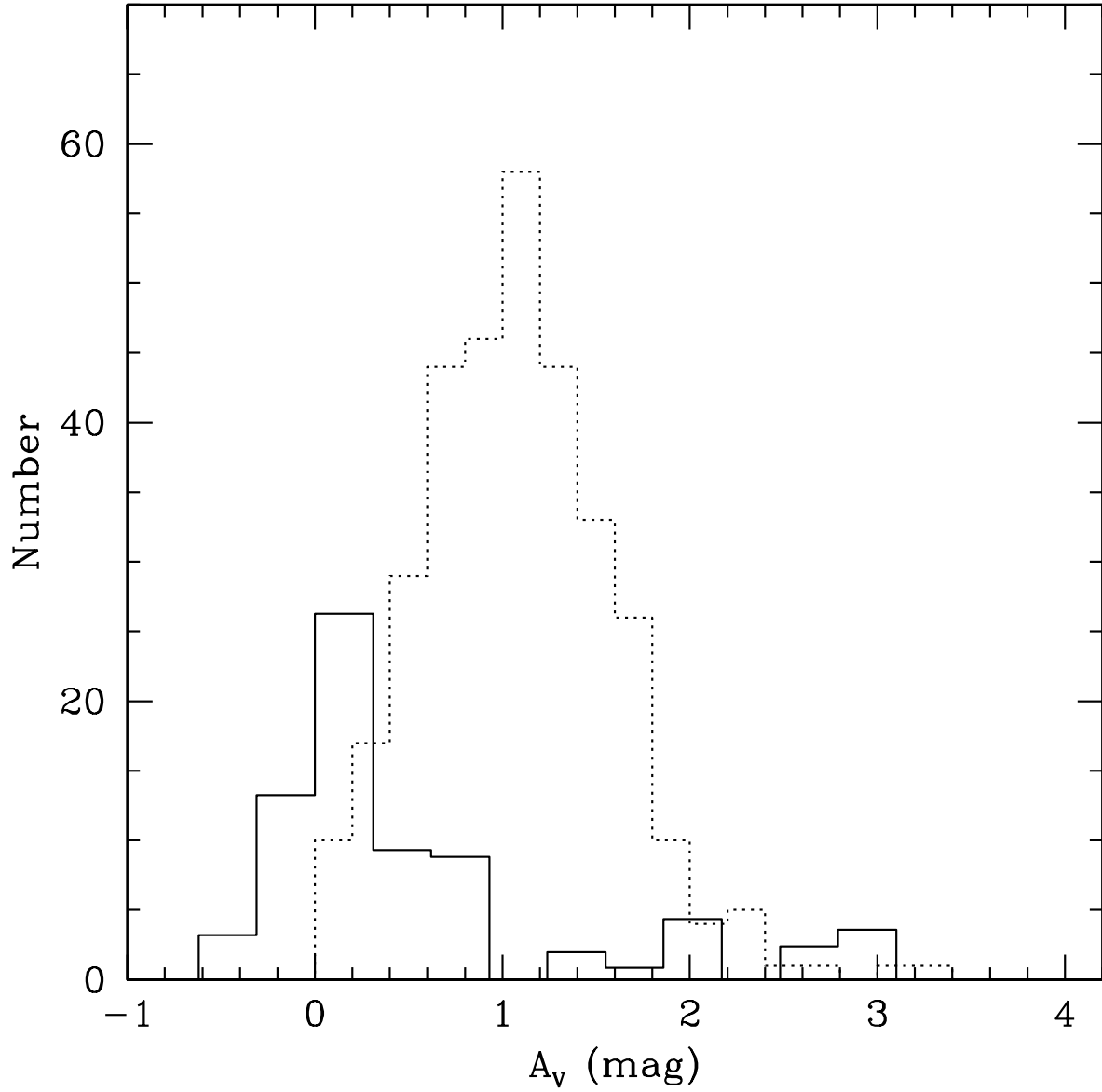


Fig. 6.— Distribution of V -band extinction A_V for SNe Ia, estimated assuming that their colour excess is due to dust reddening and $R_V = 3.1$ (solid histogram). The dotted histogram is A_V of field galaxies inferred from the Balmer emission line ratio $H\alpha/H\beta$ (Nakamura et al. 2004) for comparison.

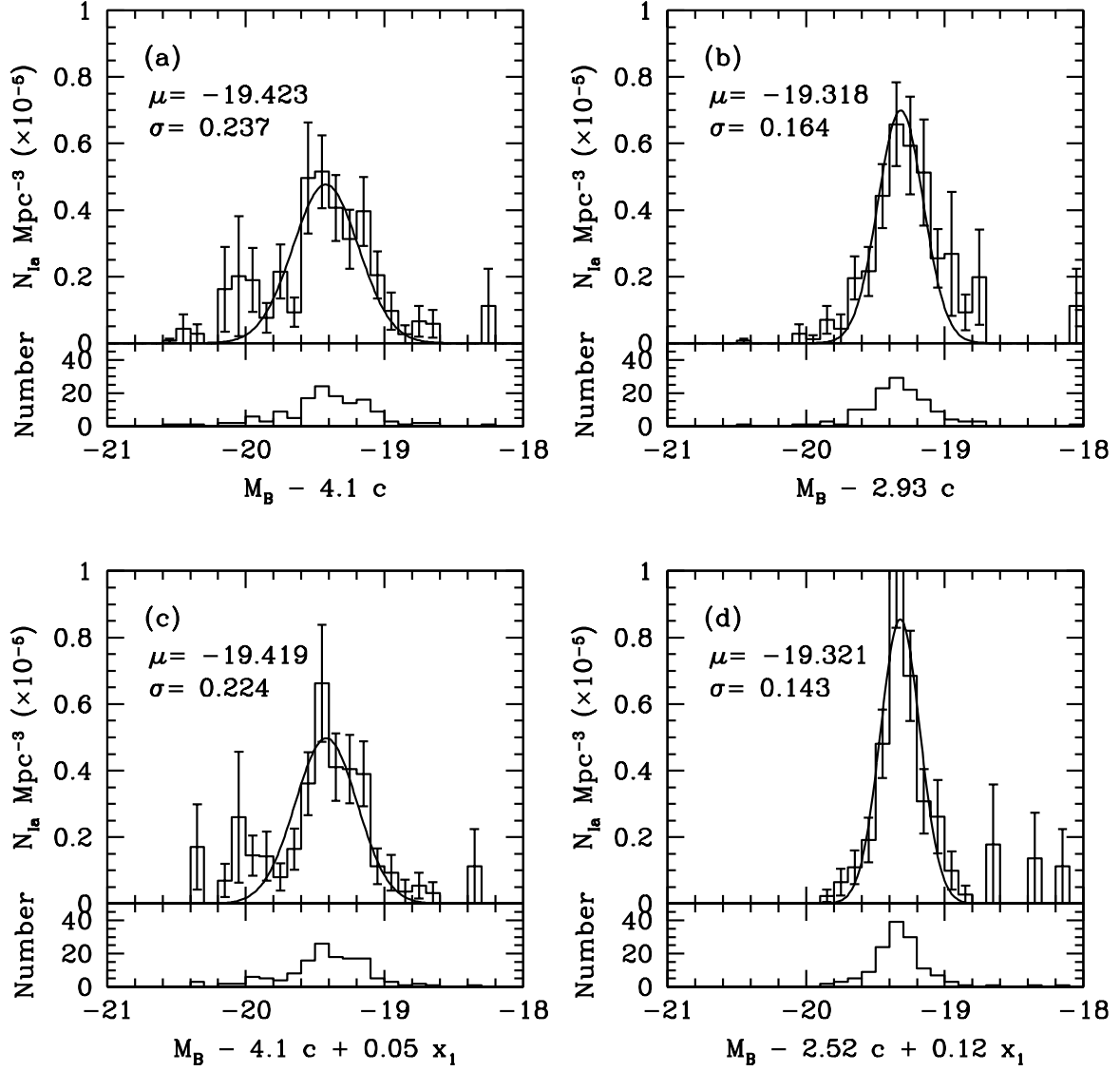


Fig. 7.— Luminosity function of SNe Ia in the B -band. B -band brightness is corrected for the colour variation as $M_B - \beta c$ ($\beta = R_V + 1$) with (a) $\beta = 4.1$ and (b) $\beta = 2.92$ which minimises the width of fitted Gaussian. The parameters of the Gaussian are shown in each panel. In panels (c) and (d) a correction for light curve shape x_1 is also taken into account with the parameter to minimise the Gaussian widths.

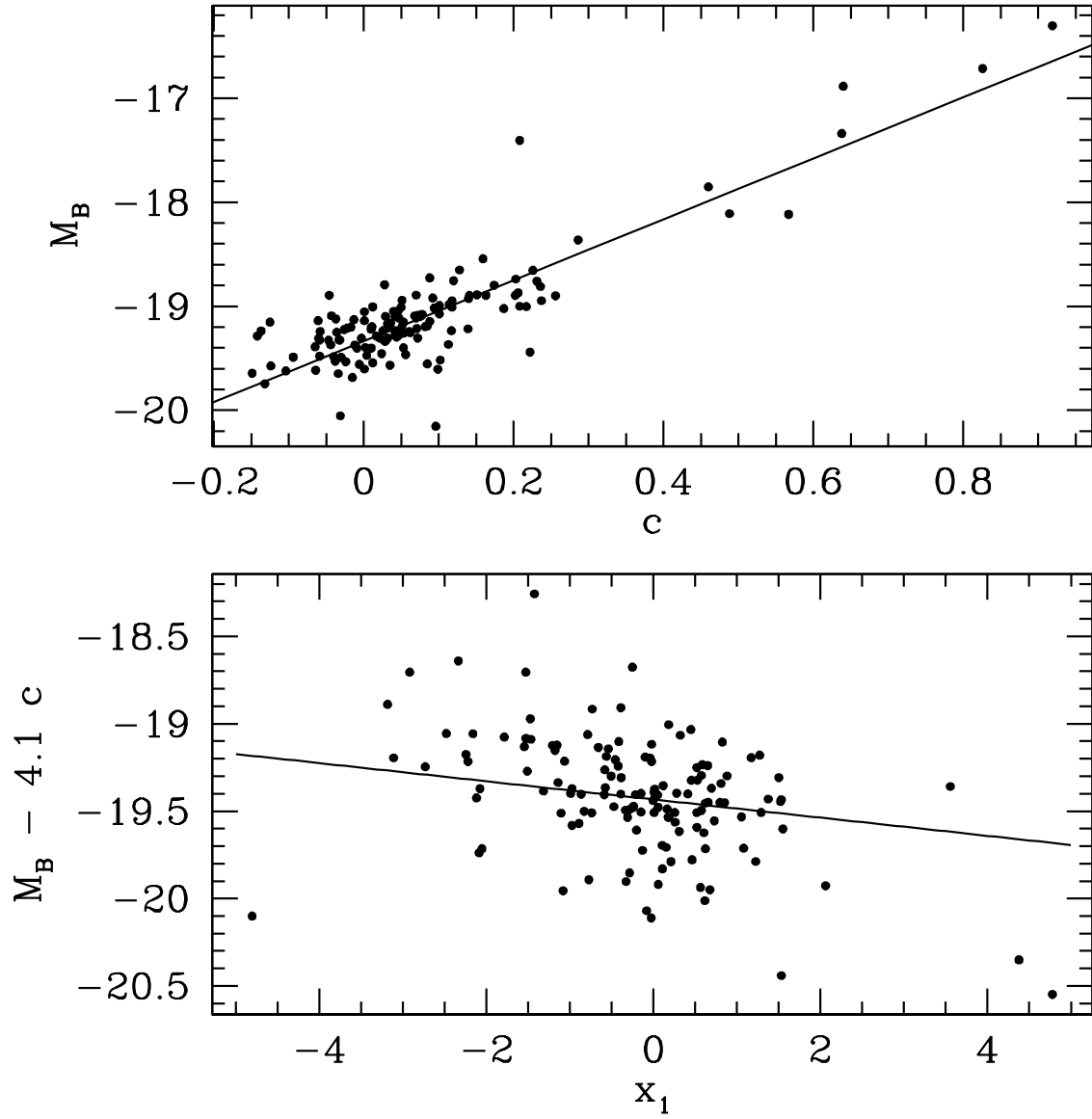


Fig. 8.— Correlations between brightness of SNe and the colour excess parameter c (the top panel) and the x_1 parameter (the bottom panel).

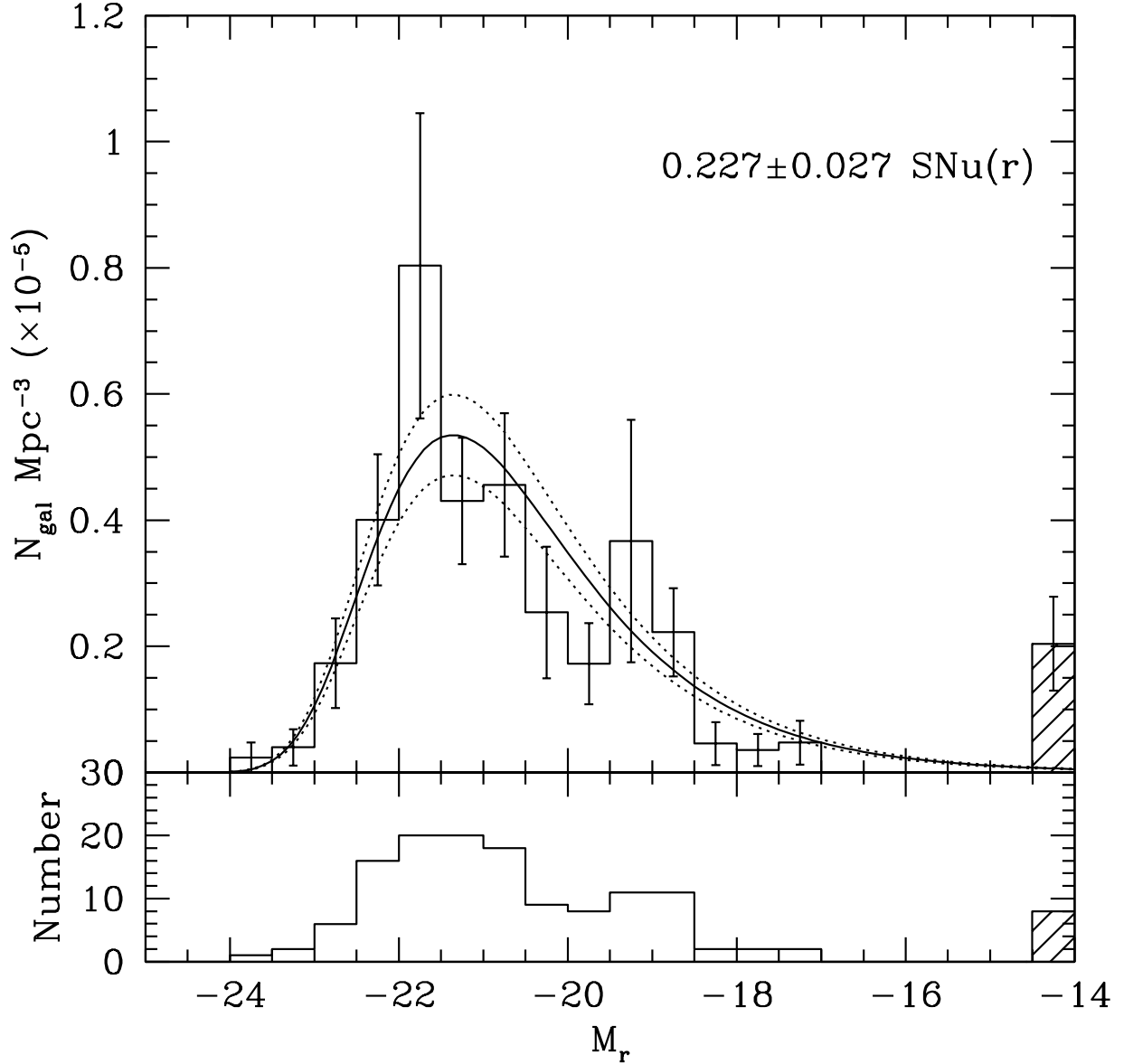


Fig. 9.— Luminosity function of SNe Ia host galaxies in the r -passband. Lower panel shows the number of contributing galaxies in each bin. The solid curve is the luminosity weighted luminosity function of field galaxies (Blanton et al. 2001) normalized to fit the histogram. The scale factor that gives the supernova rate in SNU is given at the top right of the figure. Dotted lines show the range corresponding to the fitting error. Contribution from hostless SNe are indicated in the rightmost bin with shades.

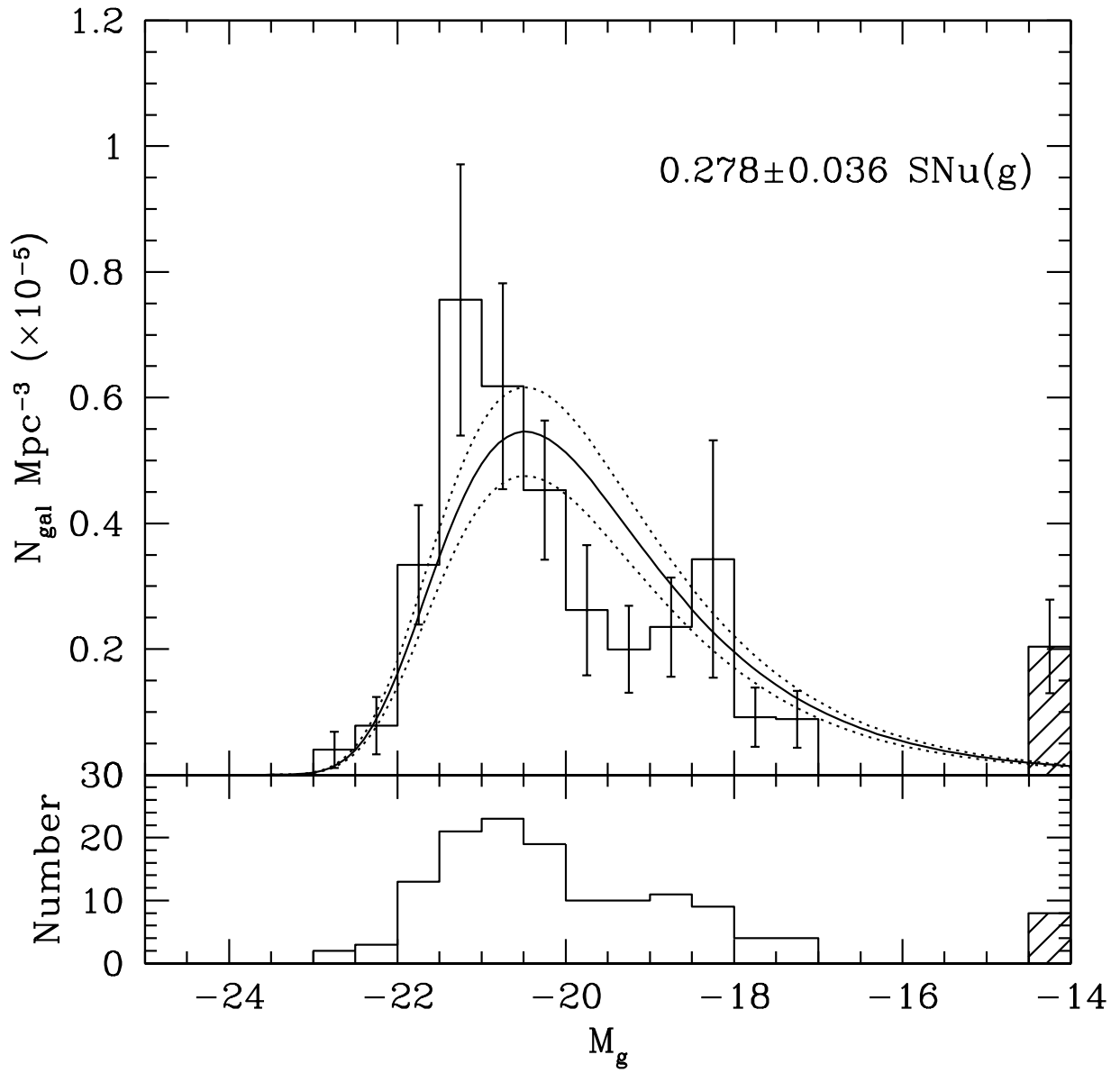


Fig. 10.— Same as figure 9 but in the g -passband.

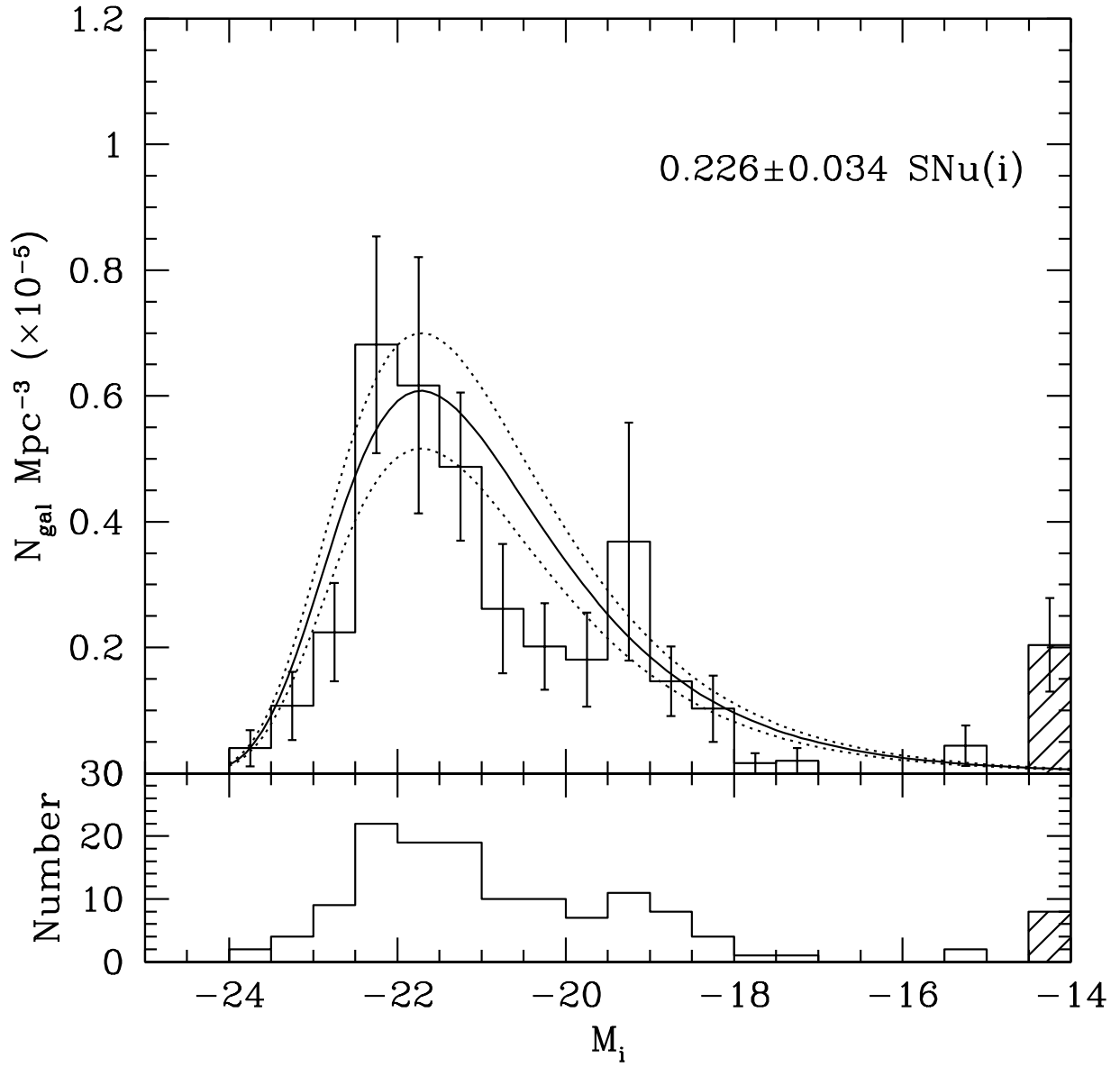


Fig. 11.— Same as figure 9 but in the i -passband.

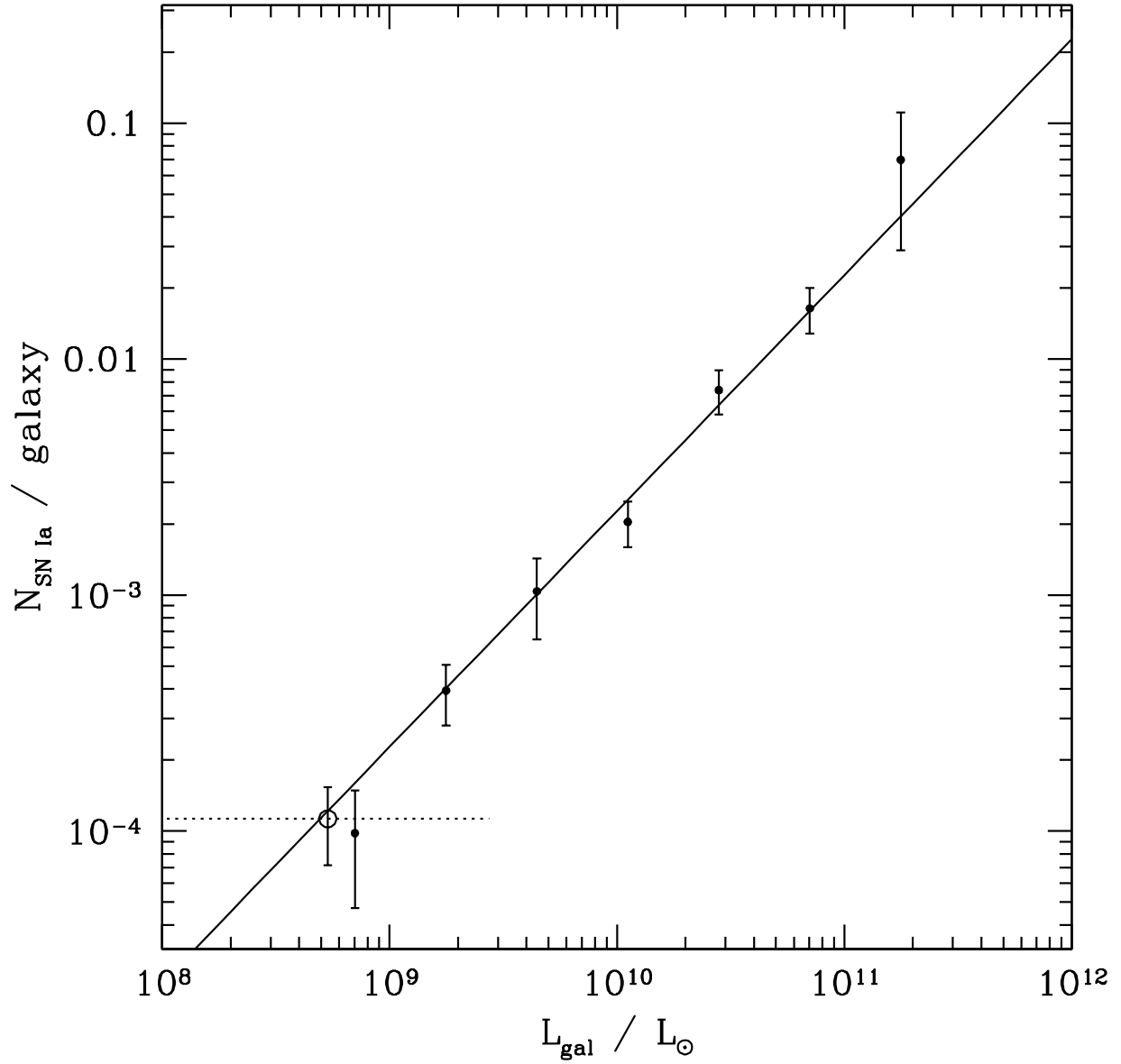


Fig. 12.— SN Ia rate per galaxy as a function of r -band luminosity of galaxies. The point denoted by the open symbol stands for the hostless SNe Ia and the horizontal bar shows the upper limit of luminosity of galaxies.

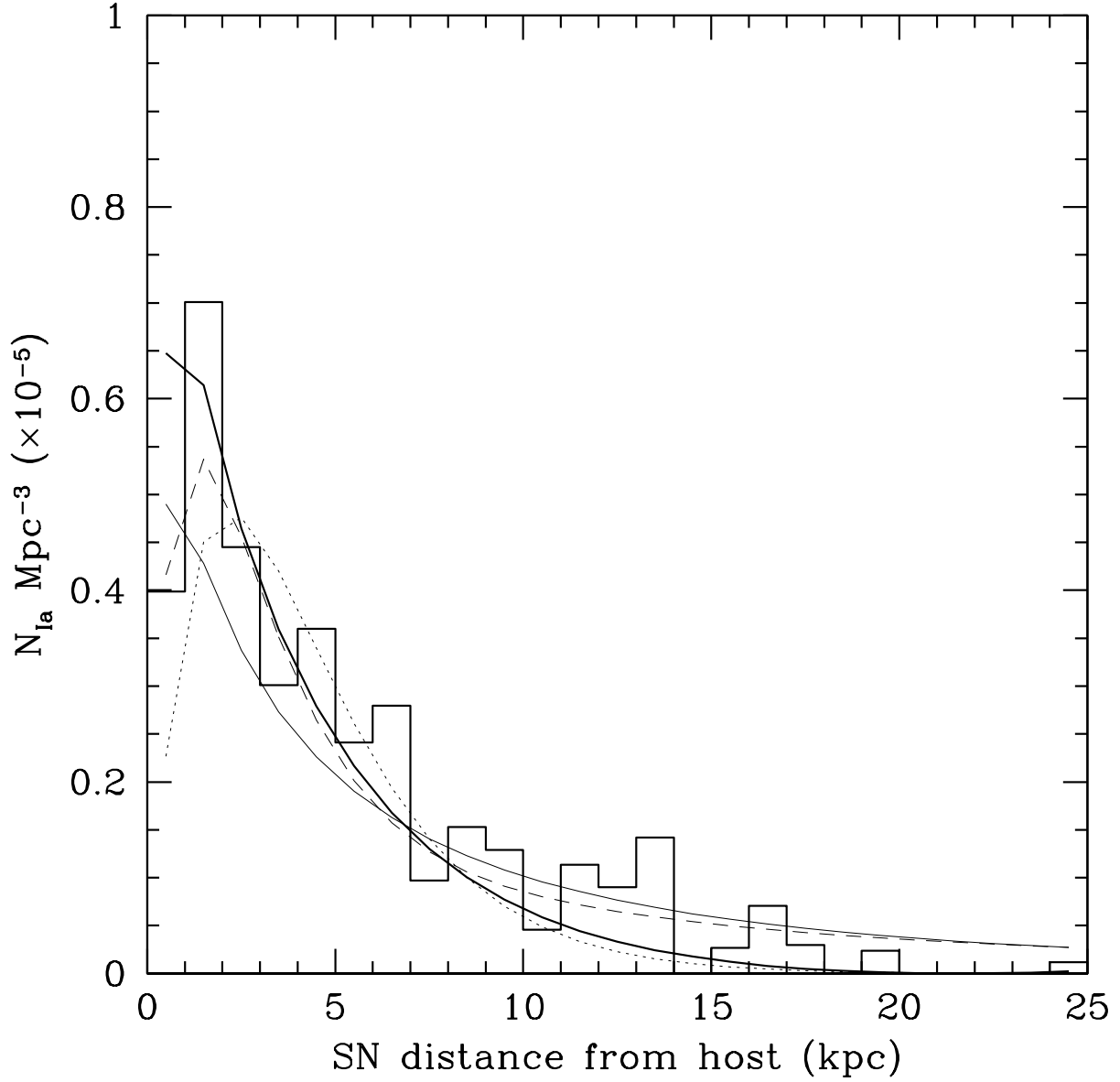


Fig. 13.— Radial distribution of SNe Ia from the centres of their host galaxies measured in physical distance scale. The thin solid, dotted and dashed lines are best fit models with de Vaucouleurs, exponential profiles and sum of these two profiles, respectively. The thick solid line is the mean r -passband galaxy light profile averaged over field galaxies.

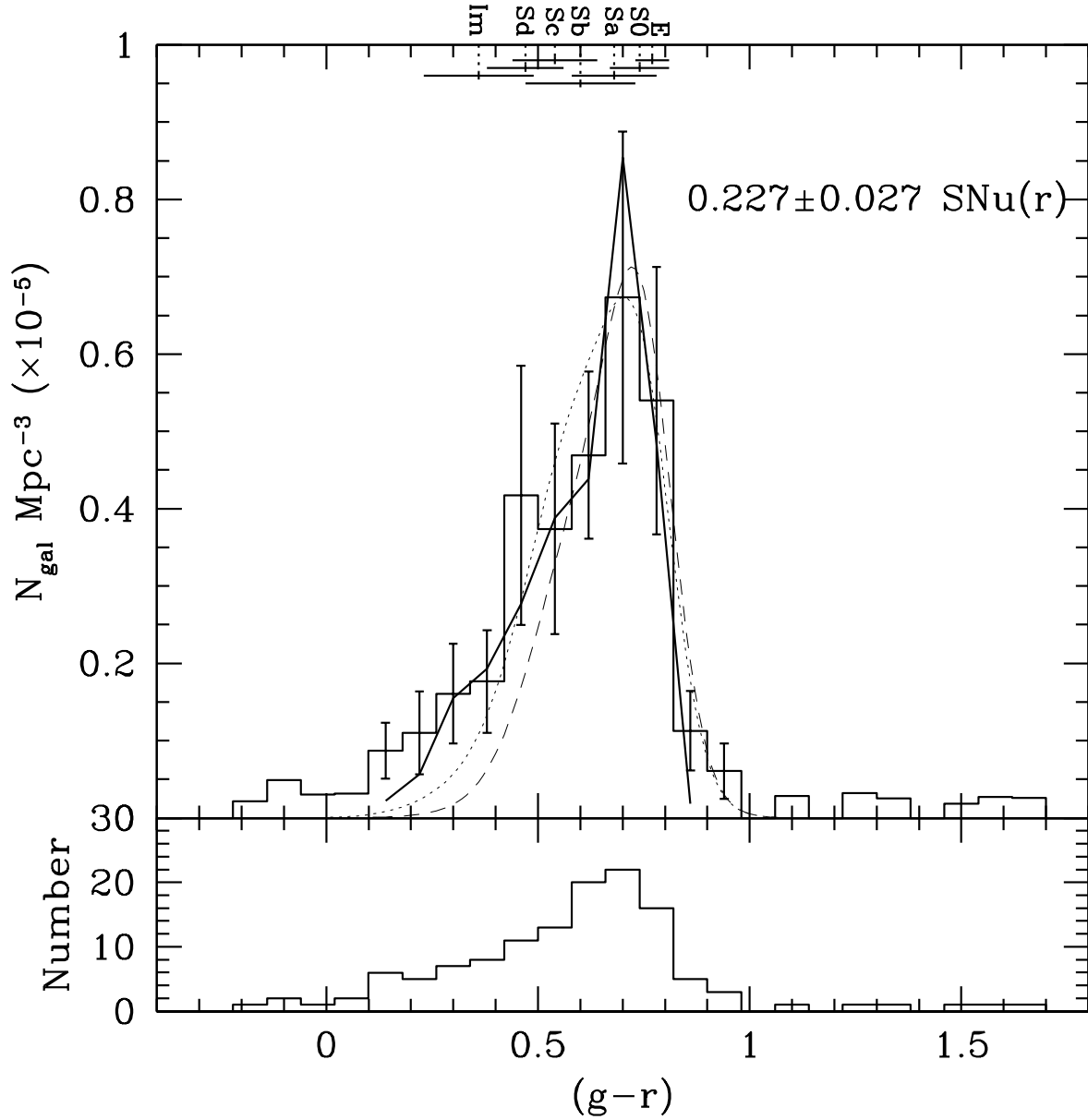


Fig. 14.— $g-r$ colour function of SNe Ia host galaxies with the lower panel indicating the number of contributing galaxies in each bin. Solid curve represents the luminosity weighted galaxy colour function normalized in the way same as in Figure 9. Morphological types of galaxies are indicated at the corresponding colours according to Fukugita et al. (2007). Horizontal bars indicate the variance within the morphological types. Dotted and dashed lines are numbers expected for SNe Ia based on the SNe Ia rate model of Mannucci et al. (2005) and Sullivan et al. (2006), respectively.

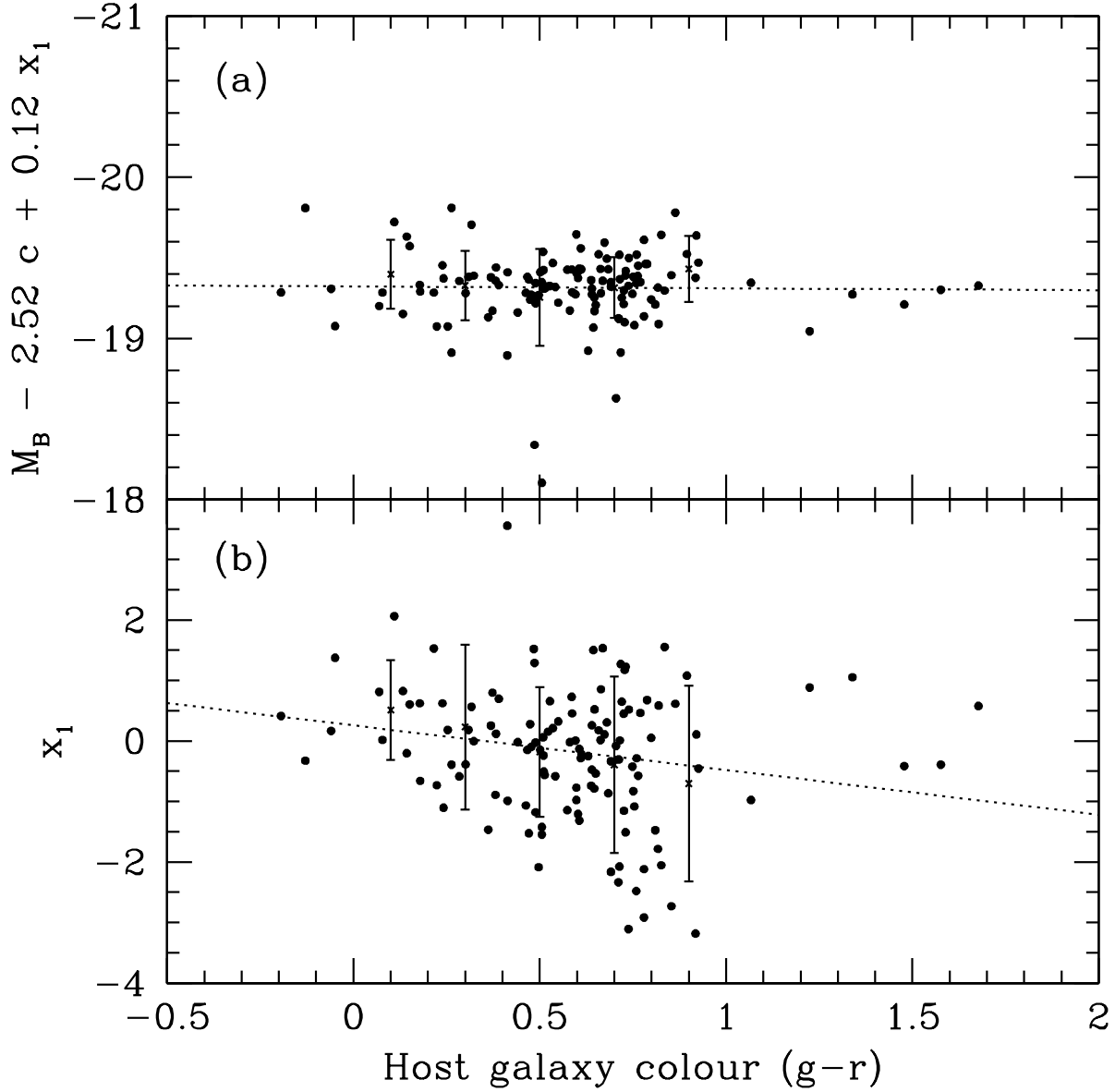


Fig. 15.— (a) Absolute brightness of SNe Ia corrected for the colour excess using $\beta = 4.1$ as a function of $(g - r)$ colour of host galaxies. The mean and dispersion of the points are also plotted. (b) Shape parameter x_1 that depends on colour $(g - r)$ of host galaxies. Dotted lines show least square fits to the data, $M_B - 4.1c = -19.32 + 0.01(g - r)$ for (a), and $x_1 = 0.26 - 0.74(g - r)$ for (b), respectively.

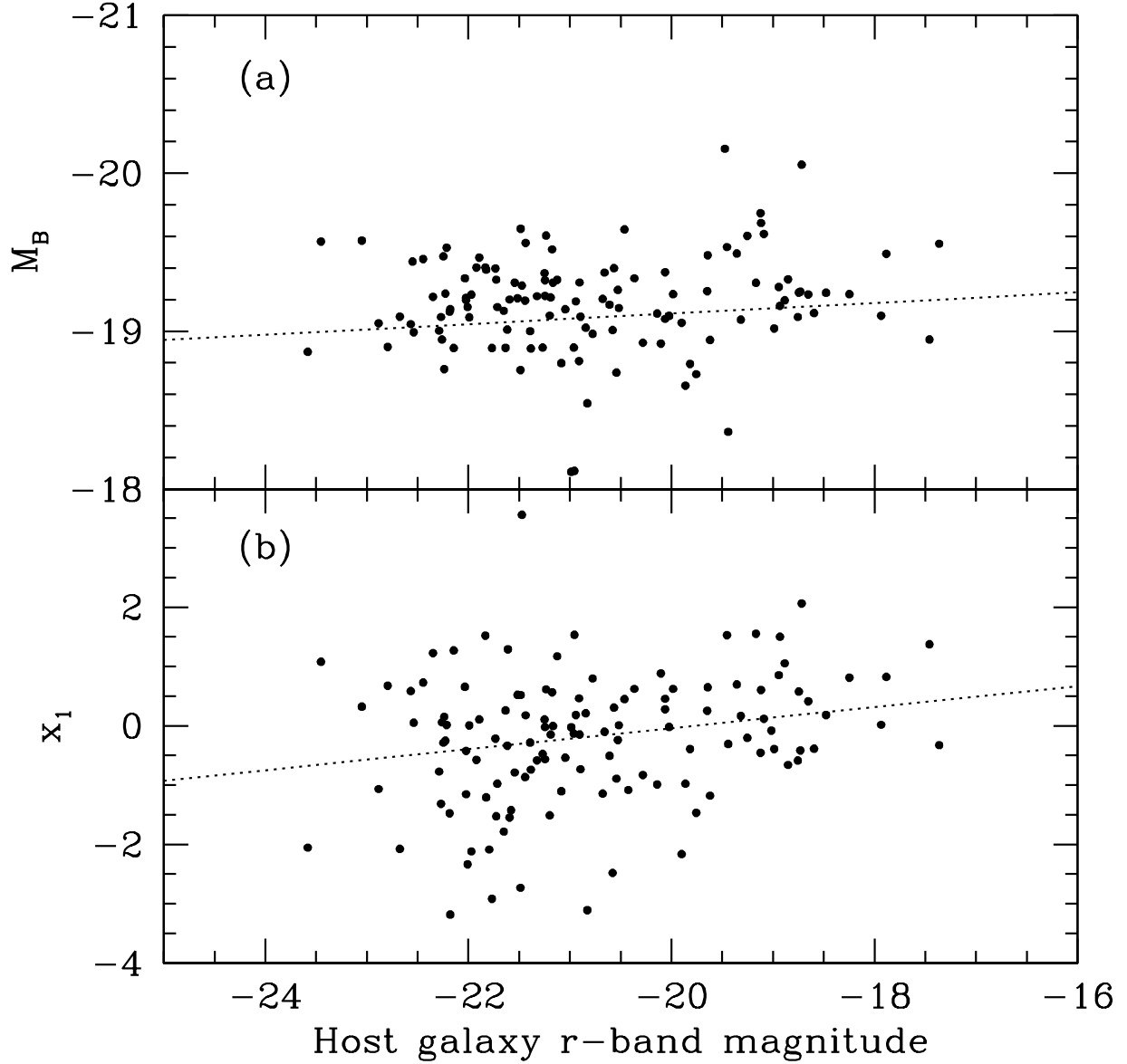


Fig. 16.— (a) Absolute brightness of SNe Ia corrected for the colour excess using $\beta = 4.1$ and (b) shape parameter x_1 as a function of r -band brightness of host galaxies. Dotted lines show least square fits to the data, $M_B - 4.1c = -19.78 - 0.034M_r$ for (a), and $x_1 = 3.50 + 0.18M_r$ for (b), respectively.

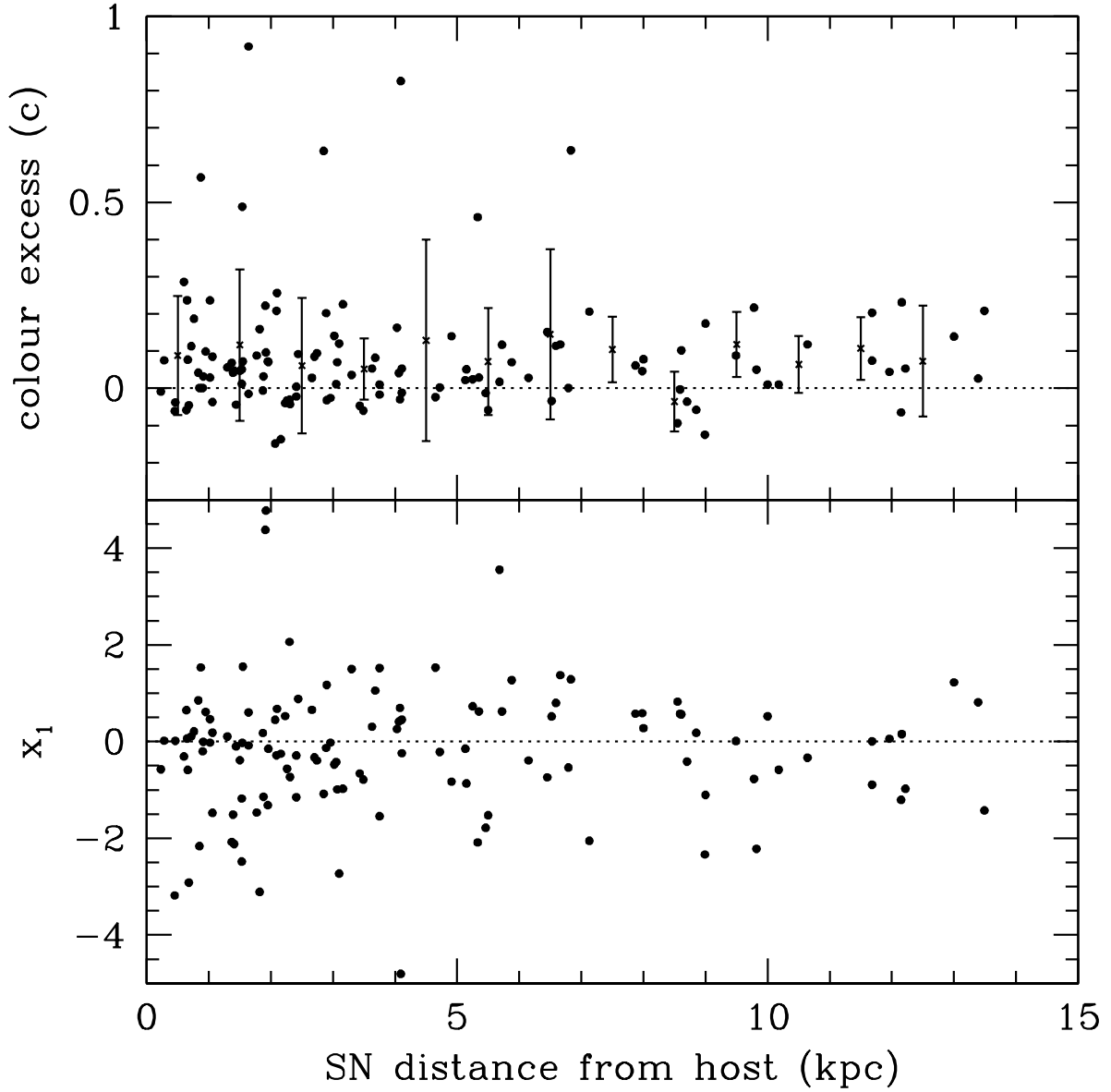


Fig. 17.— Colour excess and the x_1 parameters plotted against the physical distance of SNe Ia from the centre of host galaxies. Dotted lines indicate the zero level. In upper panel the mean and dispersion in respective bins are also plotted.

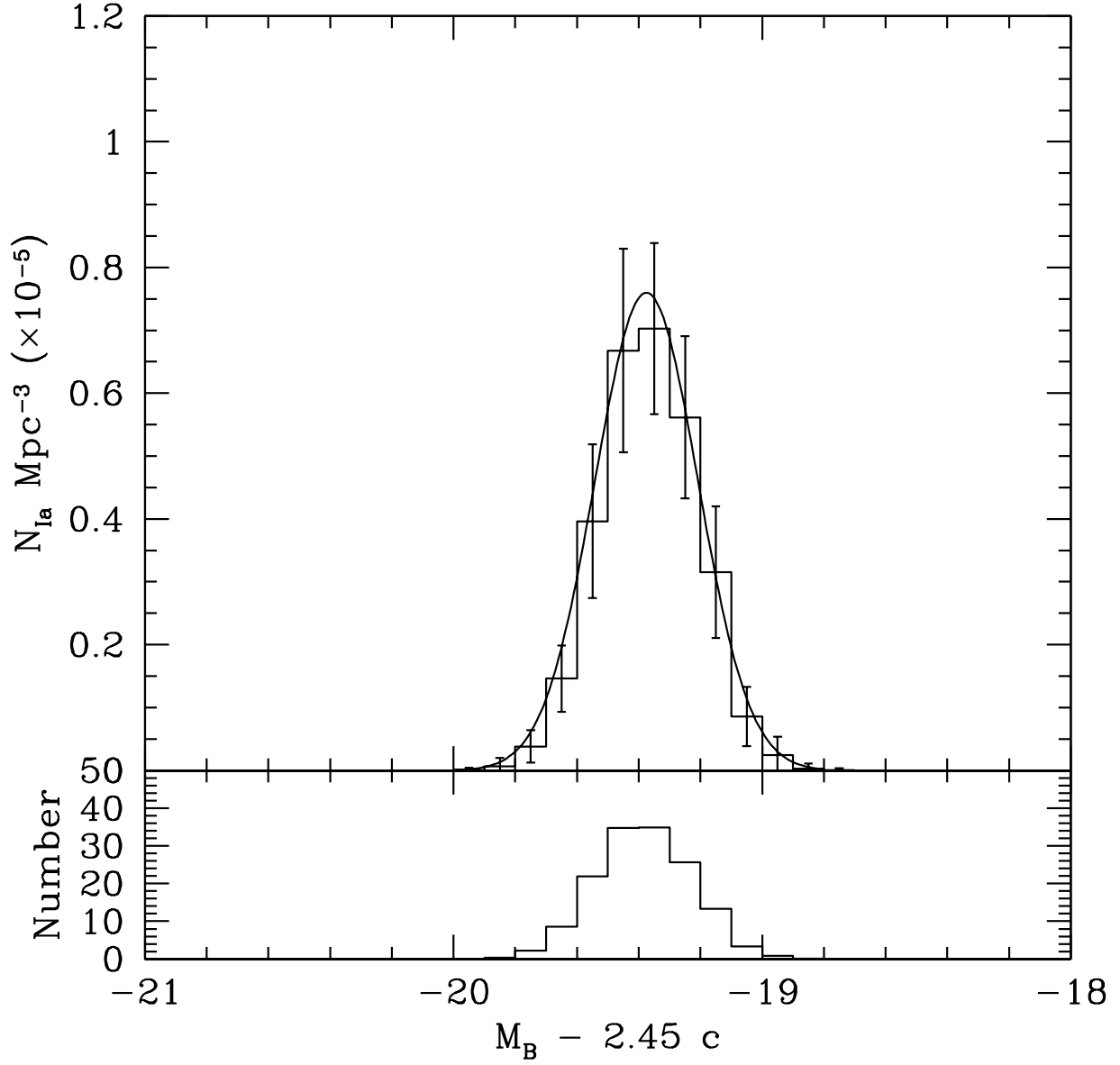


Fig. 18.— Comparison of the input SN LF (solid curve) and output SN LF (histogram) from simulated dataset assuming the completeness as a function of redshift. Histogram passes through the mean and error bars show the dispersion in each bin calculated from 50 simulation dataset.

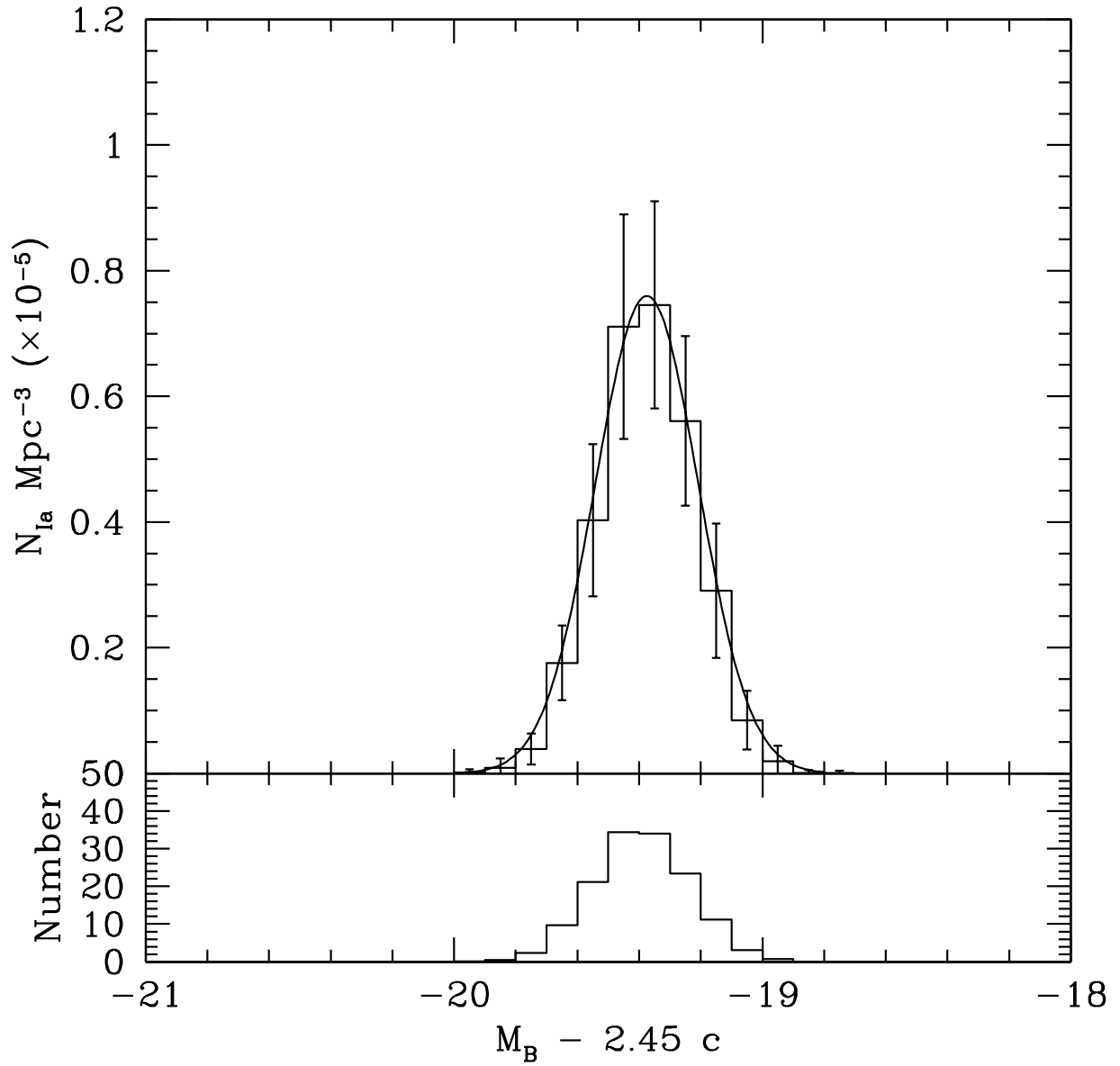


Fig. 19.— Same as Fig. 18 but completeness is assumed to be a function of apparent peak r -band magnitude.

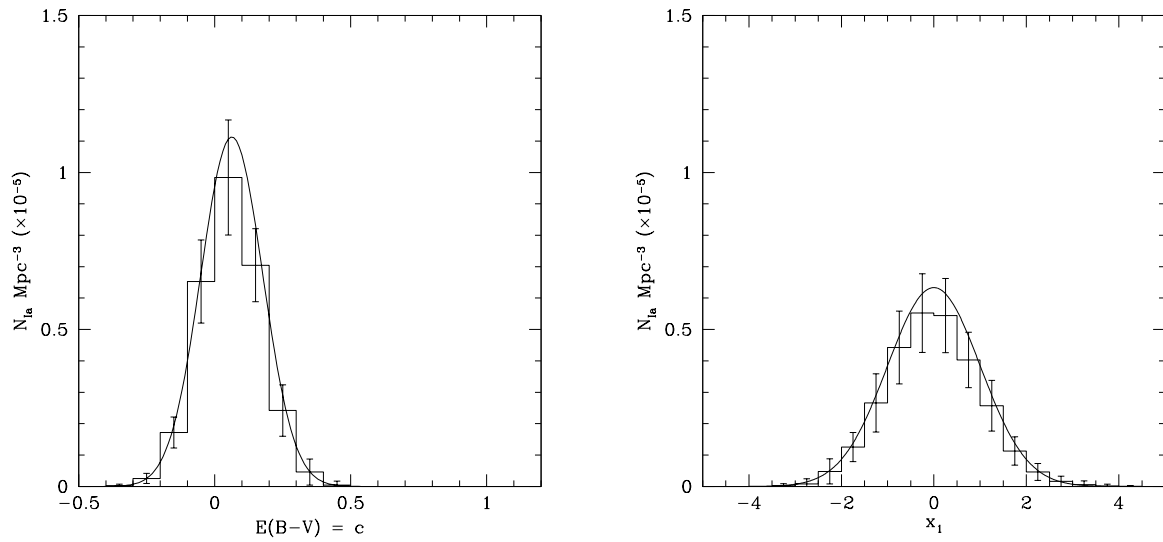


Fig. 20.— Same as Fig. 18 but for the distribution of the $E(B - V) = c$ parameter (left) and the x_1 parameter (right).

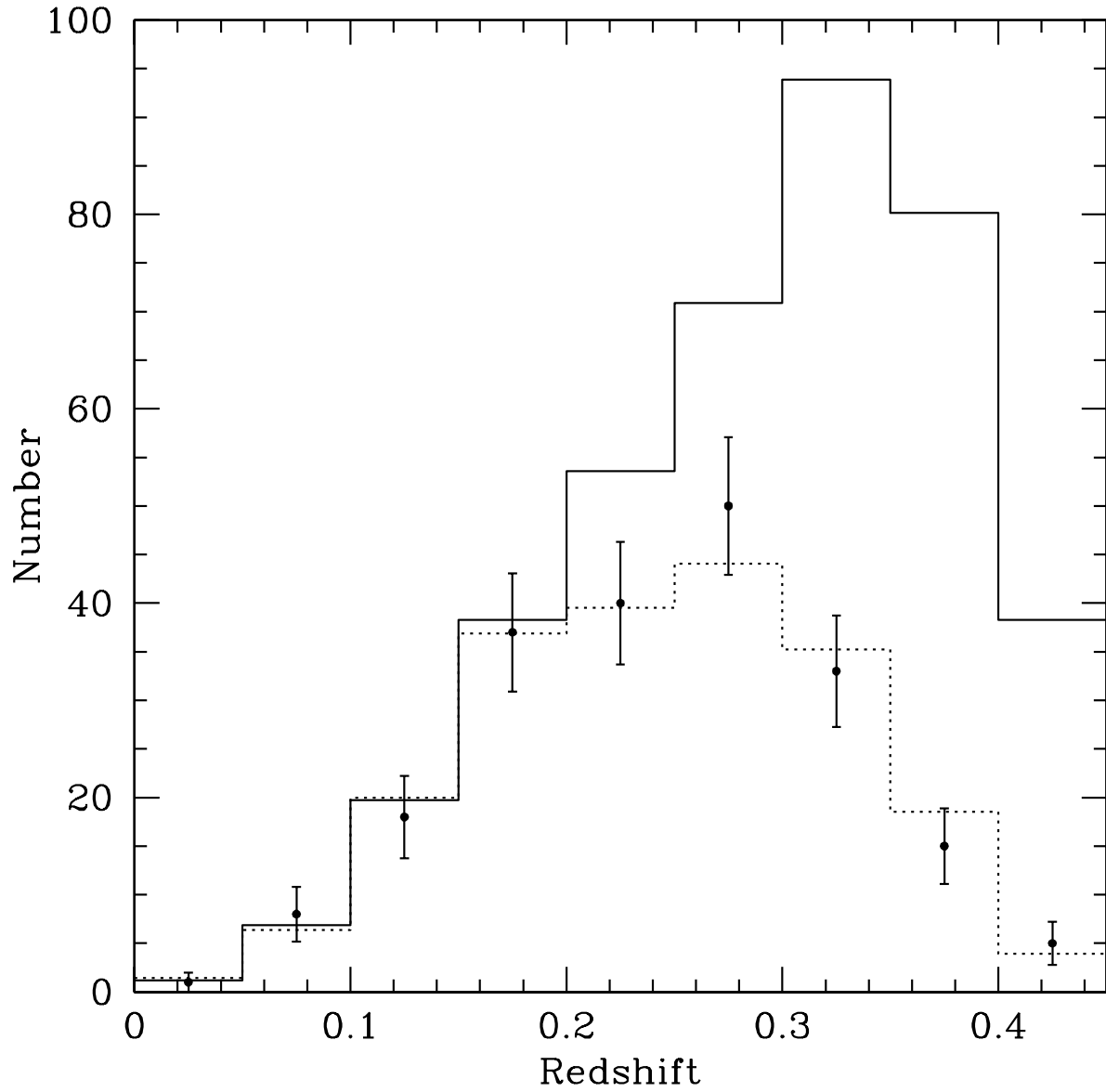


Fig. 21.— Simulated redshift distributions before (solid) and after (dotted) spectroscopic incompleteness is applied. Points with error bars represent observed SNe sample.